AN EXPERIMENTAL INVESTIGATION OF OBLIQUE WING STATIC AEROELASTIC PHENOMENA

by

Basil S. Papadales, Jr.

Thesis submitted to the Graduate Faculty of the
Virginia Polytechnic Institute and State University
in partial fulfillment of the requirements for the degree of

MASTER OF SCIENCE

in

Aerospace and Ocean Engineering

APPROVED:

T. A. Weisshaar, Chairman

E. M. Cliff

J. A. Schetz

April 1975

Blacksburg, Virginia

ACKNOWLEDGMENTS

The author wishes to thank Dr. T. A. Weisshaar for his continued support and guidance during the past year. Further thanks are extended to Mr. D. N. Bodell for building the various models and Mr. H. W. Dawson for assisting during the wind tunnel testing. Special thanks are in order for Ms. W. M. Hylton for her typing the manuscript. Finally, the author wishes to thank his wife, Rosamond, for her constant understanding and patience during the duration of this research effort.

TABLE OF CONTENTS

LIST OF FIGURES

LIST OF FIGURES - continued

LIST OF TABLES

NOMENCLATURE

b	wing span, m (ft)
c	wing chord, m (ft)
$C_{( )}$	aerodynamic coefficient
$F(x)$	general function
l,m,n	moments, Nm (lb-ft)
q	dynamic pressure, N/m^2 (lb/ft^2)
S	wing area, m^2 (ft^2)
x_i	general variable (i = 1, 2, ...)
X,Y,Z	forces, N (lb)
α	angle of attack, deg
δ_a	aileron deflection, deg
ε	strain, μcm/cm (μin/in)
$\Delta( )$	error

1. INTRODUCTION

Since the first successful aircraft flight, the outward appearance of aircraft has gone through very few drastic changes. In the early years, there was a shift from wooden biplanes to metal monoplanes. Then, after World War II, as the quest for higher speeds continued, there was a definite trend toward swept wing planforms. Finally, within the past decade, the concept of the variable sweep wing has gained moderate acceptance.

Conventionally designed variable sweep wings (Fig. 1a) employ two distinct wing panels each rotating about its own pivot. This rotation is symmetric about the longitudinal axis of the aircraft. This type of wing offers significant operational advantages. The entire aerodynamic character of the aircraft can be altered by simply rotating the wing. The obvious advantage is that high aerodynamic efficiency can be obtained throughout a large flight envelope. At low speeds the wing is unswept, thus giving the aircraft a low induced drag because of the high aspect ratio. At high speeds the wing is swept back, thus increasing the drag divergence Mach Number. Superior maneuverability is also possible since the wing span can be changed during a flight maneuver; hence a near optimal configuration can exist throughout the maneuver.

The variable sweep concept has not been fully accepted by designers because of several major disadvantages. Symmetrically sweeping the wing causes the center of gravity to move aft; with large sweep angles this travel can be quite large. Although the wing aerodynamic center also moves aft, a difficult stability and control problem results because the distance between the aerodynamic center and the center of gravity is reduced. There is also a large weight penalty incurred with this type of wing. The wing pivots exposed to very large loads, and therefore, must be quite substantial. Then too, the variable sweep wing is not a continuous structure (as a conventional wing is); hence, another weight increase must be accepted. Finally, the lowest possible drag can not be achieved for the entire flight envelope since the fuselage can not be properly area ruled for every sweep angle. For these reasons, very few aircraft using symmetric variable sweep wings have entired production; all are combat aircraft.

In 1972, R. T. Jones (Ref. 1) again proposed an alternative variable geometry wing concept which he claimed would yield at least as good aerodynamic performance as the conventional variable sweep wing. This wing (Fig. 1b) has a continuous structure which rotates about a single pivot point; thus, half the wing rotates forward, the other half rearward. This type of wing is called a yawed, skewed,

slewed, or oblique wing. There are several problems with the oblique wing, not the least of which is that aeroelastic considerations point to the disturbing fact that symmetrically sweptforward wings tend to diverge at relatively low speeds.

When an elastic wing creates lift, the wing bends upward. The equilibrium position of the wing will be where the elastic forces caused by the structural deformation exactly balance the aerodynamic forces. If the wing is deflected from this equilibrium position, two sets of pertubation forces are induced; these are aerodynamic and structural (or elastic) forces. The latter forces tend to restore the wing to the equilibrium position. The aerodynamic forces may or may not be of a restoring nature. If the incremental aerodynamic forces tend to move the wing further away from the equilibrium position and are greater than the elastic forces, then a phenomenon called "wing divergence" results.

To understand how a form of wing divergence, termed bending divergence, might occur in a clamped oblique wing, consider the oblique wing in Figure 2. Assume the wing is flexible with a straight elastic axis A-B and that the wing is clamped at the root section. On the sweptforward panel consider two cross-sections cutting the wing perpendicular to A-B; these are C-D and E-F. When a dynamic pressure is

applied, the wing tips will deflect upward if there is a positive absolute angle of attack of the mean aerodynamic chord. For simplicity, assume the wing untwisted and at some positive angle of attack so that every local wing section is exposed to a positive lift increment. Suppose the wing is exposed to some steady dynamic pressure. Section E-F, which is outboard of C-D, will deflect upward more than C-D. Since both sections are perpendicular to the elastic axis, the deflections of the points along each section must be equal; that is, the deflection of point C must be equal to that of D but less than that of E or F. The relative positions of C-D and E-F will be determined by the wing structure and the magnitude of the applied dynamic pressure. At each section the aerodynamic and structural forces will be balanced.

Now assume the spacing of the two segments is such that segment D-E is parallel to the free stream. This section must have an angle of attack greater than that of the root since the leading edge, E, is displaced more than the trailing edge, D. This condition will result in increased lift (assuming the section does not stall). Some dynamic pressure will exist where divergence will occur; that is the wing bending divergence dynamic pressure. At this point the static deflection per unit load will increase without limit. The increased load comes from the increased angle of attack.

The same argument can be used concerning the sweptback portion of the wing except that, in this case, the streamwise section will have an angle of attack somewhat less than that of the root, thus making it more difficult for the wing to diverge.

Another kind of divergence also exists; this is torsional divergence. This is a result of the relative location of the aerodynamic center being ahead of the elastic axis in most conventional wings. An increase in angle of attack increases the moment about the elastic axis causing the wing to twist so as to increase the angle of attack further. Equilibrium is reached when the aerodynamic moment is balanced by the internal wing torsional moment. Again, some dynamic pressure will exist where the structure will diverge. Torsional divergence is very dependent upon the flight Mach Number of the aircraft. If the free stream velocity is supersonic, the aerodynamic center will move aft from the quarter chord and, in general, will be behind the elastic axis. This situation can not lead to divergence in an unswept wing since an increase in dynamic pressure will result in a reduction in the angle of attack of the section. This twist is caused by the nose down moment about the elastic axis induced by the aerodynamic lift force.

Diederich and Budansky (Ref. 2) studied the divergence properties of symmetrically swept and unswept wings. They

assumed a wing clamped at the root with its sectional bending stiffness varying with the fourth power of the local chord. Linearized aerodynamic strip theory was also assumed. Their results show that torsional divergence is only a problem with wings having little or no sweep (either forward or aftward) and only if the aerodynamic center is ahead of the elastic axis. Furthermore, the wing sweep angle has a very strong effect on the divergence speed. Sweptforward wings display a decreasing divergence speed with increasing sweep angle. Wings with moderate sweepback will not diverge.

Implicit in this analysis are two important assumptions. First, the aerodynamic theory used can not account for wing tip losses and stall. The wing tip forces will be somewhat less than predicted with strip theory. Also, the aerodynamic forces will not continually increase with increasing angle of attack. Instead, at some point some sections will stall and lose lift. Second, the wing was assumed clamped at the root and fully constrained against all rigid body motion. Since the bending deflections of the two wing panels on an oblique wing can significantly differ, the bending moments can not always be equal. Since the root section can not roll under the assumed conditions, it must absorb the difference in the two root bending moments. With a real aircraft this rolling moment could not be absorbed. To maintain level flight a control or similar input would be

required or the wing structure could be designed to keep the root bending moments equal. In any case, a drag or weight penalty would be incurred. This roll equilibrium problem only occurs with unsymmetrically swept wings since a symmetrical wing would have equal and opposite root bending moments.

The problems of tip losses, stall, and roll equilibrium have not been extensively studied for the oblique wing case. The tip loss and stall problems are simply a matter of using more realistic aerodynamic models. The roll equilibrium problem is more involved. An oblique wing aircraft, with a full six degrees of freedom, will tend to bring itself into roll equilibrium by unloading the sweptforward panel until the root bending moments are equal. If the vehicle were constrained in pitch and no control input is applied, the wing will try to achieve this goal by rolling about its longitudinal axis until a bank angle is reached where the moments are equal. At this bank angle the angle of attack of the wing is less than that of the wing if it were level. Hence, for a given flight speed, the wing has been unloaded and the wing loading reduced. For an unconstrained aircraft a more complicated motion would result. The effect of this motion would be to reduce the wing loading as in the constrained case. For a flying aircraft such a reduction in wing loading is unacceptable since the loading must remain

constant for level flight. Therefore, the wing must be geometrically or structurally modified, or a control input applied.

Three solutions to this problem have been proposed. The sweptforward wing panel could be stiffened. Or, the wing could be given an initial favorable deflection which would balance the moments. Finally, an aileron deflection could be used. In all these cases a performance penalty, either from drag or weight, would result.

To predict the size of the penalties involved the magnitude of the roll control problem must be known. The degree to which roll control is a problem is determined by the flexibility of the wing. The clamped divergence speed is also strongly influenced by the wing flexibility. A low divergence speed would indicate that roll control would become important at a low speed. Hence, the clamped divergence characteristics of an oblique wing are of interest to the aircraft designer.

Preliminary research in this area has shown that for a real aircraft (which is free to roll and pitch) the wing bending divergence speed will never be reached. Instead, another aeroelastic instability, wing flutter, will occur and at a higher speed than the clamped divergence speed. Jones and Nisbet (Ref. 3) have shown this for oblique wings using analytical techniques. Wing flutter is a dynamic

instability which involves the mass and stiffness properties of the wing.

The goal of some more recent research efforts was to predict the magnitude of the roll control problem by analyzing the clamped divergence characteristics of oblique wing designs. Furthermore the flutter speeds are of interest since an oblique wing would have to maintain roll control and avoid flutter throughout its flight envelope. No experimental data was readily available with which to compare analytical results. To this end, a wind tunnel test program was conducted to gather data on several oblique wing designs. This paper presents the results of this effort.

2. FACILITIES AND MODELS

2.1 Wind Tunnel

All models were tested in the VPI&SU Stability Wind Tunnel. The general design of this facility is shown in Figure 3. The test section is 1.83 m (6.0 ft) square and 7.02 m (23.0 ft) long. All models were sting mounted and supported by a pylon vertically spanning the tunnel downstream of the test section. In this configuration, a maximum dynamic pressure of 1650 N/m^2 (34.5 lb/ft^2) was obtainable. The model angle of attack could be varied from a control outside of the test section. The pylon was equipped with a compensating traverse mechanism which automatically centered the model in the test section at the angle of attack selected. Further details of this facility can be found in Appendix A.

2.2 Wind Tunnel Models

The wind tunnel models were designed to minimize cost and fabrication difficulties while using existing equipment to the fullest extent. A variety of wing models were constructed from aluminum and steel sheet metal. All the wings models had a flat plate airfoil section. These wings were attached to one of two centerbodies especially designed and constructed for this test program. One centerbody housed a strain gage balance system and held the wing

firmly clamped at the root. The other centerbody was substantially smaller and also clamped the wing at the root. This body, however, was free to roll about the sting support.

2.2.1 Wing Models

A total of 23 wings were constructed. Each had an area of 0.1131 m^2. (1.22 ft^2). The characteristics of each wing are listed in Table 1. These wings were consecutively numbered for identification. The wings were divided, by planform, into three groups. The first group (Wings 1-10) had an untapered planform. This planform had the wing tips aligned with the free stream for all sweep angles (Fig. 4). This provided a series of wings which could be exactly modelled for analytical purposes. Since the tip shape was dependent on the sweep angle, a different wing had to be constructed for each sweep angle to be tested. Wings were built for 0, 30, and 60 deg sweep. All of these wings were constructed from 0.163 cm (0.064 in) thick aluminum sheet and had a structural span of 1.20 m (3.94 ft^2). The unswept aspect ratio was 12.7.

The second planform group (Wings 11-19) had a linearly tapered planform with a taper ratio of 0.50. The wings had the same structural span as the untapered wings. These tapered wings, however, were designed to partially simulate actual aircraft wings, and therefore, had a fixed planform

(independent of the sweep angle). These wings had a straight quarter-chord line. The wings were designed to be tested at sweep angles of 0, 15, 30, 45, and 60 deg. One wing with this design was constructed from the same aluminum as the untapered wings, another from 0.183 cm (0.072 in) thick steel, and a third was constructed with a steel sweptforward panel and an aluminum sweptback panel. The latter design was intended to study the effect of stiffening the swept-forward panel.

Both the untapered wings and the tapered wings were designed to be rotated about the root quarter-chord line. The wings were clamped parallel to the centerbody longitudinal axis and through this point.

Ailerons were simulated on each of the above wings by cutting into the trailing edge of the wings in two places on each semiwing and bending the metal between the cuts to simulate a plain flap aileron. All the wings had the ailerons located between 60 and 90% of the semispan; the aileron chord was 25% of the local wing chord. To eliminate a variety of problems, a separate wing was constructed for each aileron angle tested. Aileron angles of 0, 3, and 6 deg were tested, so three wings of each planform or material design had to be constructed. Wings with zero aileron deflection also had similar cuts in order to maintain structural uniformity among the wings.

All wings were rotated with the right wing panel (viewed from the top) rotated forward; therefore, the ailerons were deflected asymmetrically with the right aileron up. This would be the proper deflection to bring the wing into roll equilibrium.

The final group of wings (20-22) had an elliptical planform. Two of these had pure elliptical distributions about a straight quarter-chord line. These wings had aspect ratios of 10.6 and 12.7. Rotation was about the quarter-chord line. These were the original oblique wing planforms proposed by Jones (Ref. 3).

A third wing was constructed with a modified elliptical planform of aspect ratio 12.7 (Wing 22). This planform (Fig. 4) differed from the pure elliptical designs in that it had more wing area concentrated at the root. This design has the properties of minimal induced drag and a constant root bending moment when unswept (Ref. 4). This wing design had a straight 40% chord line and was rotated about this chord line.

All of the elliptical wings were designed to be tested at sweep angles of 0 to 60 deg in 15 deg intervals. All of these wings were constructed from the same aluminum as the others and had aileron cuts located as on the other wings, but no aileron deflection was used.

A strain gage was mounted to each of the wings with zero aileron deflection (Wings 1, 5, 8, 11, 14, 17, 20, 21, and 22). The gages were mounted 15 cm (5.9 in) outboard from the root and along the elastic axis. All the wings gaged, except the untapered 30 deg sweep wing (Wing 5), had a single uniaxial gage mounted on the lower surface of the right (sweptforward) wing panel. This one wing had a gage mounted on both the sweptforward and sweptback panels.

Finally, the unswept untapered aluminum wing (Wing 1) was copied so that two identical wings were available. Wing 1 had a strain gage mounted; Wing 2 did not. This provided a control test case to determine what effects the strain gage would have on the behaviour of the wings.

2.2.2 Centerbodies

As stated previously, two centerbodies were used. The primary body, designated Centerbody A, was 140 cm (55.1 in) long and 9 cm (3.5 in) in diameter. This body was not free to roll and housed the ST01 strain gage balance system. The wings were rotated about a point 70 cm (27.6 in) aft of the nose; the balance was centered at this point. The body was designed with an ogive nose and boat-tail. A 5.0 cm (2.0 in) diameter steel rod connected the balance and plyon. The boat-tail section was designed to completely clear this support so that the only contact between the balance or support members and the centerbody was at the balance mount.

Details of this centerbody are shown in Figure 5.

A second centerbody, B, was designed to be free to roll. This body was 70 cm (27.6 in) long and 5.0 cm (2.0 in) in diameter. A rigid 2.5 cm (1.0 in) diameter rod was connected to the same rod used to support the ST01 balance. Two roller bearings were located along this smaller stainless steel rod. A brass tube was fitted over the bearings and the wings clamped to it. The body had a small ogive nose. A simple mechanism was included that could lock the outer tube in a position in which the wings would be level. A machine screw was passed through the outer tube and threaded into the center rod. Two such screws were provided for extra strength. This centerbody also had a small steel weight at the bottom of the body to counterbalance the wing. Details of the entire centerbody design are in Figure 5.

The wings were connected to centerbodies in an identical manner. At the pivot point a 0.625 cm (0.25 in) thick piece of steel was mounted on the body. This provided a flat surface on which to mount the wings. The wings were mounted to this with two machine screws. The wings were rotated around a large 0.95 cm (0.375 in) diameter screw; a second 0.12 cm (0.047 in) diameter screw was mounted 5.0 cm (2.0 in) aft of the first screw. The purpose of this small fastener was to insure that the wing had a specific sweep angle. Each wing, except the untapered wings, had a

series of five small holes drilled to this diameter corresponding to the various sweep angles.

A 0.320 cm (0.125 in) thick piece of steel was mounted on top of the wing to insure the root section was fully clamped. These two steel pieces were both 2.50 cm (1.0 in) wide and had rounded leading edges and sharp trailing edges. The two wing mounting screws passed through the top steel piece and the wing and were threaded into the lower piece. Details of this mounting system are shown in Figure 5.

2.3 Instrumentation

2.3.1 Force and Moment Data

Normal, Axial, and Side forces and Roll, Pitch, and Yawing moments were measured using the ST01 Strain Gage Balance. This device was housed in the centerbody (A) and measured these quantities in the body axes. Output was measured on a bank of three two-channel strip chart recorders.

2.3.2 Strain Data

Strain measurements were taken by means of a bridged strain indicator. This device, once set with the proper gage factor, gave readings directly in microcentimeters per centimeter. For all the gaged wings, except the wing with two gages, the active wing gage was directly connected to the indicator. A compensating gage bonded to a small piece

of wing material was mounted to the underside of the centerbody and was fully exposed. Two compensating gages were used; one mounted to aluminum, the other to steel. All the strain gages used came from the same manufacturer's lot to ensure consistent quality.

When two active gages were used, a simple circuit was connected in which the output from either active gage could be connected to the strain indicator through a double throw switch. The same compensating gage was used for both active gages.

2.3.3 Miscellaneous Data

The tunnel dynamic pressure was measured through a pitot static tube mounted approximately 50 cm (19.7 in) ahead and 45 cm (17.7 in) above the models in the test section. Pressures were measured by meaning of an electronic manometer and digital voltmeter. The angle of attack of the centerbodies could be measured by means of a counter mounted near the wind tunnel controls. Output was proportional to the angle of attack.

3. EXPERIMENTAL PROCEDURE

3.1 Clamped Tests

A majority of the tests were conducted using Centerbody A. For these tests the centerbody and balance were mounted in the test section. For each wing configuration, measurements were made at five different dynamic pressures and at one angle of attack. For all but one test sequence, the angle was 4.00 deg. The range of dynamic pressures differed greatly between different wings and sweep angles since the divergence character of each was different. An attempt was made to conduct the tests between 50 and 90% of the expected divergence dynamic pressure.

For each test the tunnel was permitted to reach an equilibrium dynamic pressure; the strip chart recorders were then run for no less than 5 s. If the wing model had a strain gage bonded to it, the strain was recorded simultaneously with the force and moment data. All 22 wings were tested in this manner.

The first test was conducted with the two wings which had no sweep or taper (1 and 2). This was done to determine the effects of the exposed strain gages before the other tests were started. These tests were run at an angle of attack of 4.00 deg.

The only wing tested at angles other than 4.00 deg was the untapered aluminum wing with 30 deg sweep (Wing 5).

This wing was tested at angles of attack of 2, 3, and 4 deg. This same wing had the second gage mounted on the left wing panel. Data was recorded from this gage and the other at an angle of attack of 4.00 deg. Force and moment data were only taken at this angle of attack also.

3.2 Unclamped Tests

For these tests Centerbody B was mounted in the test section. Only three wings were tested with this centerbody. The first tests used the tapered aluminum wing with 6 deg aileron deflection (Wing 13). Tests were conducted at an angle of attack of 4.00 deg and at sweep angles of 30 and 45 deg. The strain was measured at various dynamic pressures with the centerbody locked and free to roll. When the body was unlocked, the wing had to be supported until the tunnel dynamic pressure was large enough to stabilize the wing. At low speeds the ailerons would not be balanced by the aeroelastic rolling moment, and the wing would tend to roll. Since there were wires leading from the strain gage to the sting, the centerbody had to be prevented from continuously rolling at these lower speeds. This was done by means of a rod passing through a small hole in the side of the test section. The rod could be manipulated from outside the section walls. To support the wing, the rod was placed under the right (sweptforward) wing, thus stopping any positive rolling. Again, at every test dynamic pressure,

the tunnel was permitted time to come to an equilibrium pressure before measurements were recorded.

A second set of unclamped tests were conducted with the untapered aluminum wings with 30 deg of sweep. These wings had aileron deflections of 3 and 6 deg (Wings 6 and 7). Each of these wings were mounted on Centerbody B at a variety of angles of attack between 0 and 6 deg. For each angle of attack, the tunnel dynamic pressure was adjusted until the wing/body combination was level. This was done at ten different angles. Another ten tests were conducted in which the dynamic pressure was set and the angle of attack adjusted until the wings were level. In each case, the angle of attack and dynamic pressure were the only data recorded.

No precise method was available to determine the wing roll angle. Observations made through windows in the side and top of the test section were used to determine when the wings were level. Tests were run between 5.0 (0.104) and 1400 N/m (292 lb/ft^2) dynamic pressure.

3.3 Flutter Tests

A final set of tests were run with the same two wings as the previous tests (Wings 6 and 7) to determine the dynamic pressure at which flutter would occur when the wings were free to roll. Centerbody B was used. Flutter dynamic pressures were recorded for each wing at angles of attack

from 0.5 to 5.0 deg in intervals of 0.5 deg. The flutter dynamic pressures were determined solely from visual observations.

The flutter dynamic pressure was not maintained in the test section for more than 10 s. This was done to avoid damaging the wings.

4. DATA REDUCTION

4.1 Force and Moment Data

The strain gage balance data from previous calibration tests was fed into a computer program designed to develop an influence coefficient matrix by means of a least squares routine. All wind tunnel force and moment data was reduced through a second computer program which applied the raw data to the coefficient matrix and resulted in pure forces and moments in the body axes. This same program reduced these data to the standard aerodynamic coefficients in the body and wind axes.

For uniformity, the nondimensional coefficients were computed using a standard set of physical dimensions. The standard dimensions were:

Area	0.1131 m^2	(1.22 ft^2)
Chord	0.09425 m	(0.309 ft)
Span	1.200 m	(3.94 ft)

Errors were computed using the Square Root of the Sum of the Squares Method. Details may be found in Appendix B.

4.2 Strain Data

The strain measurement taken during a given test was normalized by subtracting the average of the zero readings taken before and after that test. No other corrections

were made. This procedure was followed for all tests.

4.3 Miscellaneous Data

The recorded angle of attack and dynamic pressure were read directly from wind tunnel instrumentation. No corrections were applied.

5. EXPERIMENTAL RESULTS

5.1 Clamped Tests

5.1.1 Force and Moment Data

Force and moment data for each wing configuration is shown in Figures 6 through 23. Numerical data are presented in Appendix C. In all cases the lift, pitching moment, and rolling moment coefficients are presented. In general, the data for all the wings are similar. The lift and pitching moment coefficients increase with dynamic pressure. The rolling moment coefficients become more negative with increasing dynamic pressure. This is a result of the sweptforward wing bending upward with the increasing dynamic pressure. A comparison between Wings 1 and 2 (Fig. 6) showed that the exposed strain gage had a negligable effect on the aerodynamics of the wing.

At a given dynamic pressure, an increase in the wing sweep angle caused the magnitudes of the coefficients to increase. This was only true of sweep angles up to 45 deg; the forces and moments were considerably less at 60 deg sweep (Fig. 12). This was true for all the wings tested. The effect of an aileron deflection was to reduce the magnitude of the coefficients for all the wings.

The stiffening of the wing structure (by the use of steel instead of aluminum) increased the dynamic pressure at which aeroelastic problems began (Fig. 12 and 16).

Stiffening the sweptforward panel alone had about the same effect (Figs. 12 and 18).

The effect of the wing taper ratio on the aerodynamic characteristics are presented in Figure 24. It can be seen that the tapered wing had superior lift and aeroelastic characteristics compared to the untapered planform. The effect of the general planform is shown in Figure 25. The pure elliptical planform was inferior to the modified elliptical planform. The major difference between the two can be seen in the slope of the rolling moment data. Finally, the effect of the wing aspect ratio is presented in Figure 26. This data is for the two elliptical wings with aspect ratios of 10.6 and 12.7. The lower aspect ratio wing had a totally different character than the higher aspect ratio design. The sweptforward panel on the lower aspect ratio wing did not experience the bending deflections that the other wing did. At sweep angles greater than 15 deg, the rolling moment was positive (Fig. 22) indicating that the sweptback panel was experiencing greater upward deflections. The higher aspect ratio wing had slightly better low speed lift characteristics (Fig. 26).

5.1.2 Strain Data

Strain data with the wings clamped is shown in Figures 27 through 32. Numerical data are tabulated in Appendix C. With the untapered wings a seven-fold increases in strain

was recorded with a two-fold increase in dynamic pressure (Fig. 27). These data were taken very close to the wing divergence dynamic pressure. This figure shows how quickly the strain can increase when divergence is neared. The rate at which the strain increases was found to depend on the angle of attack of the wing root section; Figure 28 presents data at various angles of attack for the untapered aluminum wings. The strain was found increase more sharply at lower angles of attack.

Strain data from the sweptforward panels of the tapered wings confirmed the hypothesis that the wings experienced less aeroelastic effects at 60 deg sweep than at 45 deg sweep (Figs. 29 through 31). Strain data from the aluminum wing (with two strain gages) showed that the sweptback panel experienced little strain while swept (Fig. 32). This data, however, is somewhat suspect since the sweptback panel has greater strain at low speeds than the sweptforward panel. No explanation could be found for this.

5.1.3 Divergence Velocity

The divergence velocity for the untapered aluminum wing (Wing 5) was estimated by plotting the inverse of the lift and pitching moment coefficients and the strain versus the dynamic pressure. The data was extrapolated with a third-order least squares curve fit. The point at which the fitted functions crossed the zero line was the

divergence dynamic pressure, since at this point the lift, pitching moment, and strain would be infinite. These data are presented in Figure 33. The estimated dynamic pressure at divergence was 309 N/m^2 (6.45 lb/ft^2); the velocity was then 22.2 m/s (72.8 ft/s).

This method could be used with this wing since the data was close to the divergence speed. The last data point was at 81% of the dynamic pressure or 90% of the divergence velocity. Wind tunnel data from the other wings did not approach the divergence speed to this degree; hence, the extrapolation could not be made with confidence.

5.2 Unclamped Tests

5.2.1 Strain Data

The strain data taken with the tapered aluminum wing (Wing 13) is presented in Figure 34. The data is presented with the wing free to roll and clamped. It can be seen that the sweptforward panel was unloaded when allowed to roll freely. The difference in the strain between the clamped and unclamped cases varied as much as by ten-fold. The strain at 45 deg sweep was larger than at 30 deg sweep when the wing was clamped, but less than the 30 deg sweep case when the wing was free to roll.

5.2.2 Roll Equilibrium

Figure 35 shows the results of the roll equilibrium tests in which the angle of attack and dynamic pressure

were recorded when the wing achieved a wings-level condition with no roll rate. The product of the angle of attack and dynamic pressure is presented as a function of the dynamic pressure. The untapered aluminum wings with 3 deg and 6 deg aileron deflections were used (Wings 6 and 7). The product of the dynamic pressure and angle of attack must remain constant if a real aircraft is to maintain equilibrium flight conditions. Test results show that this product does remain nearly constant throughout a wide range of dynamic pressures and well above the clamped divergence dynamic pressure. The product does vary considerably at low dynamic pressures (high angles of attack) because of wing stall effects.

5.2.3 Flutter Dynamic Pressures

Figure 36 shows the dynamic pressures at which flutter was observed to begin for the untapered aluminum wings with aileron deflections (Wings 6 and 7). These data are plotted for various angles of attack. The flutter dynamic pressures were observed to decrease as the angle of attack increased. The decrease was greater for the 3 deg aileron deflection than the 6 deg case. It should be noted that these wings had a flat plate section which stalled at very low angles of attack (4-5 deg). Hence, the flutter dynamic pressure was nearly constant below stall angles of attack.

6. CONCLUSIONS

From the tests conducted and the observed results the following conclusions were made:

1. The use of simple flat plate wing models provides an inexpensive method for obtaining basic qualitative static aeroelastic data.

2. The only major difficulty with this technique is the low angles at which the wings stall. This phenomenon was observed to significantly lower the flutter dynamic pressures at angles of attack above 4 deg. Similar reductions have been observed with conventional aeroelastic models (Ref. 5).

3. The wing planform has a large effect on the static aeroelastic characteristics of a wing. It is preferable to concentrate as much of the wing area as possible near the root to minimize the bending moments. However, at large sweep angles (say, 60 deg) the root wing area would be blocked by the fuselage.

4. The use of ailerons does reduce aeroelastically induced characteristics. Roll control is possible throughout a wide range sweep angles since the aileron on the sweptforward panel becomes more effective with increasing sweep due to bending deformations.

5. The use of a stiff wing, or just a stiffened forward wing panel, does reduce the magnitude of the static

aeroelastically induced forces, moments, and strains.

6. For a given aileron setting, a wing with freedom to roll will maintain a wings-level condition throughout a wide range of dynamic pressures for a given wing loading.

7. An oblique wing with freedom to roll will experience flutter at speeds at or above the clamped divergence speed. Unclamped divergence was not observed.

REFERENCES

1. Jones, R. T., "Reduction of Wave Drag by Asymmetric Arrangement of Wings and Bodies," AIAA Journal, Volume 10, Number 2, February 1972, pp. 171-175.

2. Diederich, F. W. and Budansky, B., "Divergence of Swept Wings," NACA TN 1680, August 1948.

3. Jones, R. T. and Nisbet, J. W., "Transonic Transport Wings--Oblique or Swept?" Astronautics and Aeronautics, Volume 12, Number 1, January 1974, pp. 40-47.

4. Jones, R. T., "The Spanwise Distribution of Lift for Minimum Induced Drag of Wings Having a Given Lift and a Given Bending Moment," NACA TN 2249, December 1950.

5. Rauscher, M., "Model Experiments on Flutter at the Massachusetts Institute of Technology," Journal of Aeronautical Sciences, Volume 3, March 1938, pp. 171-175.

TABLES

TABLE 1

WING SPECIFICATIONS

Wing	Λ(deg)	λ	δ_a(deg)	Material	Gaged*
1	0	0	0	Al	Yes
2	0	0	0	Al	No
3	0	0	3	Al	No
4	0	0	6	Al	No
5	30	0	0	Al	Yes
6	30	0	3	Al	No
7	30	0	6	Al	No
8	60	0	0	Al	Yes
9	60	0	3	Al	No
10	60	0	6	Al	No
11	0-60	1/2	0	Al	Yes
12	0-60	1/2	3	Al	No
13	0-60	1/2	6	Al	No
14	0-60	1/2	0	St1	Yes
15	0-60	1/2	3	St1	No
16	0-60	1/2	6	St1	No
17	0-60	1/2	0	Al/St1	Yes
18	0-60	1/2	3	Al/St1	No
19	0-60	1/2	6	Al/St1	No
20	0-60	elliptic (b/c_R=8)	0	Al	No
21	0-60	elliptic (b/c_R=10)	0	Al	No
22	0-60	modified ellipse	0	Al	No

*All wings with strain gages had a single gage on the sweptforward panel, except wing S_i; it had gages on the sweptforward and sweptback panels.

TABLE 2

WING DIMENSIONS

Wing	Structural (unswept) Span, m(ft)	Mean Aerodynamic Chord, m(ft)	Aspect Ratio
1	1.20 (3.94)	0.0942 (0.309)	12.7
2	1.20 (3.94)	0.0942 (0.309)	12.7
3	1.20 (3.94)	0.0942 (0.309)	12.7
4	1.20 (3.94)	0.0942 (0.309)	12.7
5	1.20 (3.94)	0.0942 (0.309)	12.7
6	1.20 (3.94)	0.0942 (0.309)	12.7
7	1.20 (3.94)	0.0942 (0.309)	12.7
8	1.20 (3.94)	0.0942 (0.309)	12.7
9	1.20 (3.94)	0.0942 (0.309)	12.7
10	1.20 (3.94)	0.0942 (0.309)	12.7
11	1.20 (3.94)	0.0977 (0.321)	12.7
12	1.20 (3.94)	0.0977 (0.321)	12.7
13	1.20 (3.94)	0.0977 (0.321)	12.7
14	1.20 (3.94)	0.0977 (0.321)	12.7
15	1.20 (3.94)	0.0977 (0.321)	12.7
16	1.20 (3.94)	0.0977 (0.321)	12.7
17	1.20 (3.94)	0.0977 (0.321)	12.7
18	1.20 (3.94)	0.0977 (0.321)	12.7
19	1.20 (3.94)	0.0977 (0.321)	12.7
20	1.09 (3.59)	0.116 (0.381)	10.6
21	1.20 (3.94)	0.102 (0.334)	12.7
22	1.20 (3.94	0.110 (0.361)	12.7

All wings have an area of 0.1131 m^2 (1.22 ft^2)

FIGURES

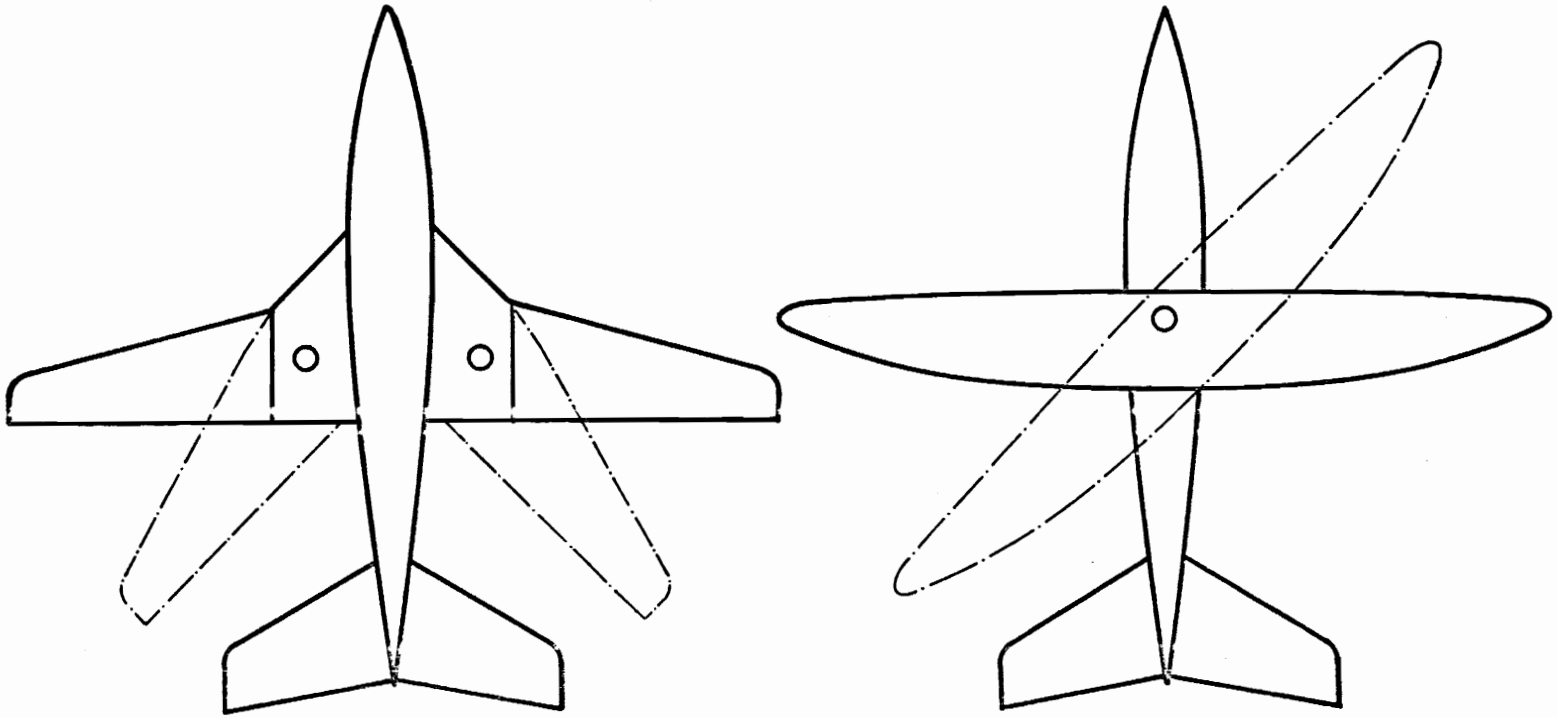

a. SYMMETRIC

b. OBLIQUE

FIG. 1 VARIABLE GEOMETRY WING CONCEPTS

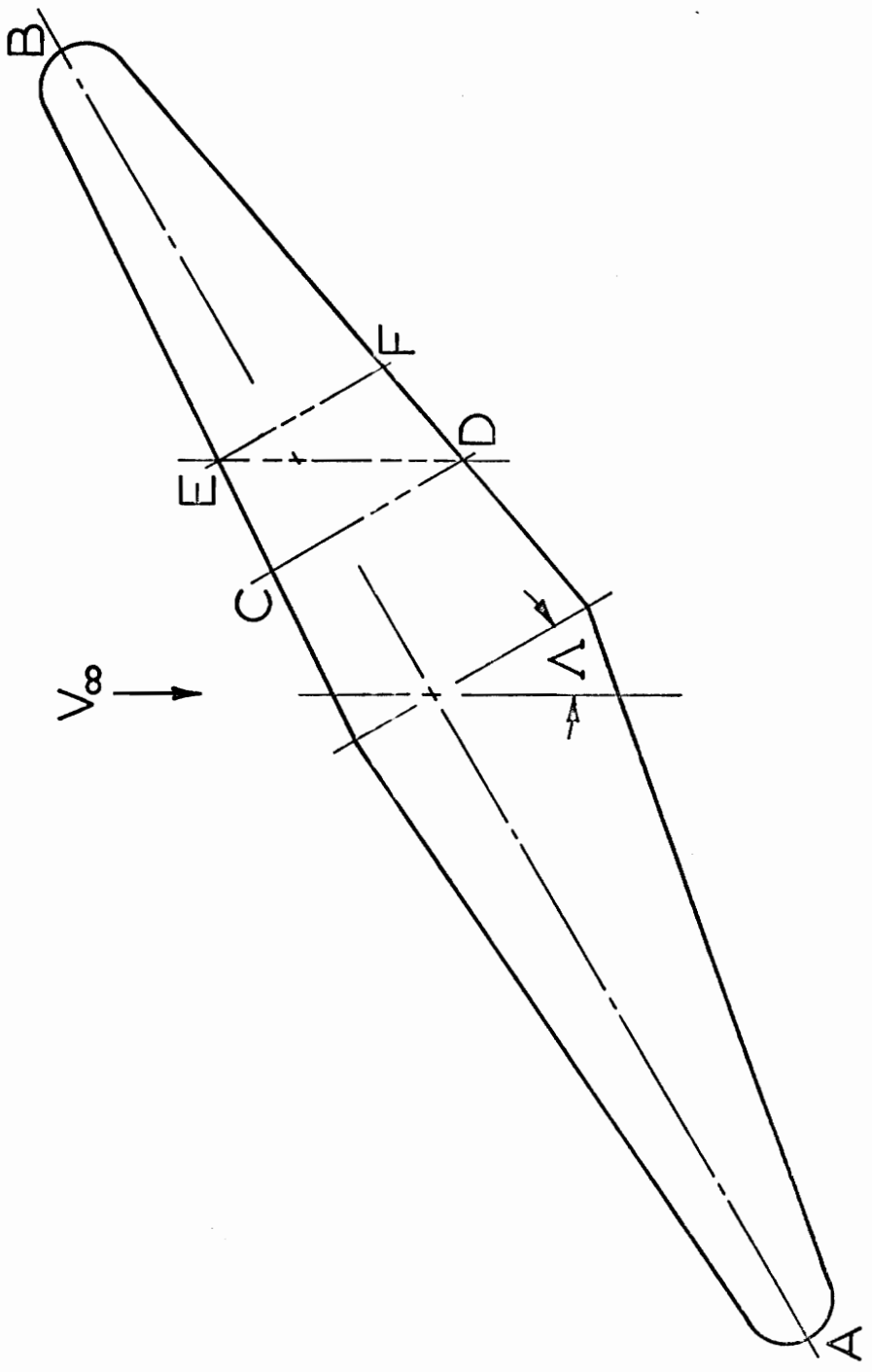

FIG. 2 THE OBLIQUE WING

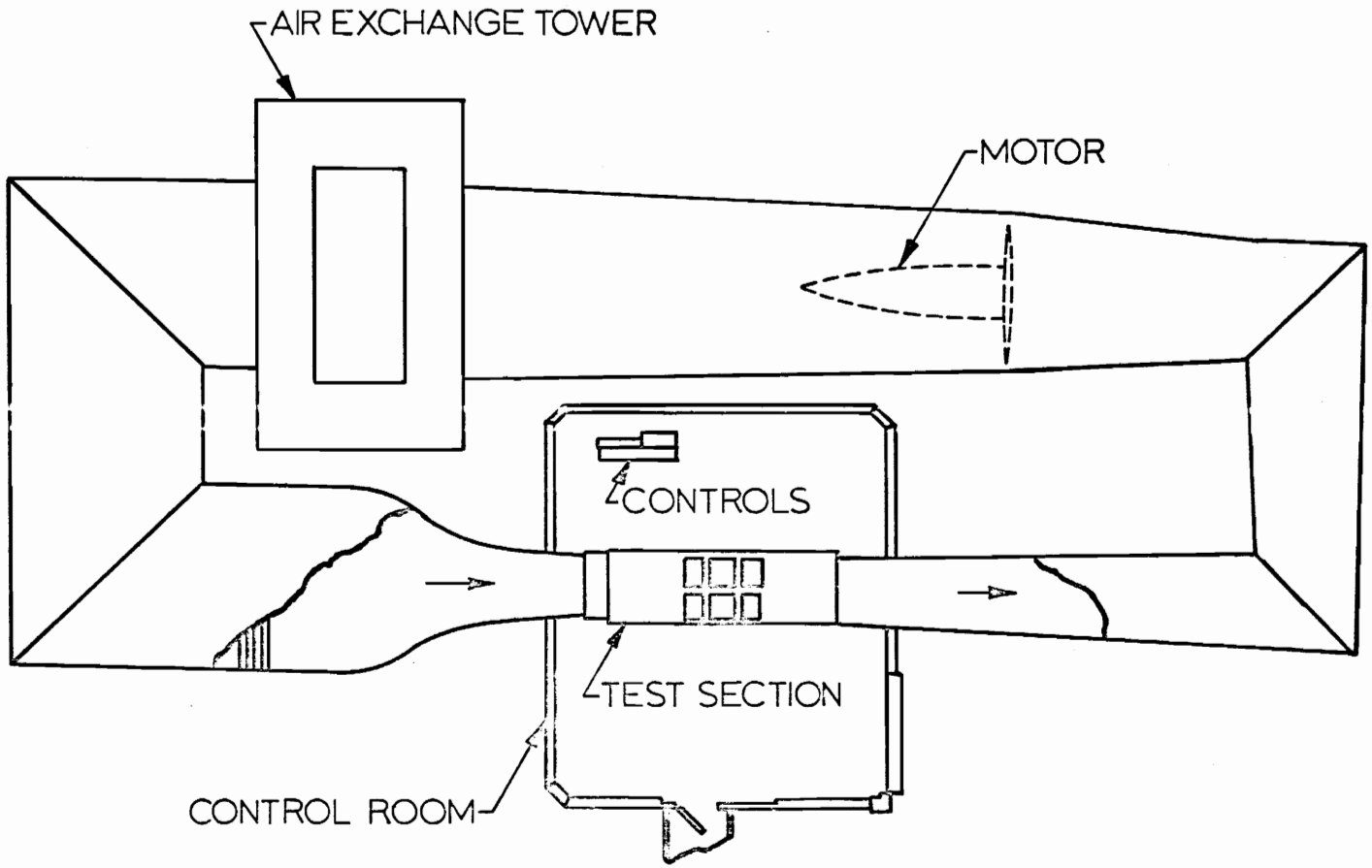

FIG.3 VIRGINIA TECH STABILITY WIND TUNNEL

PLANFORM	ASPECT RATIO	NO.
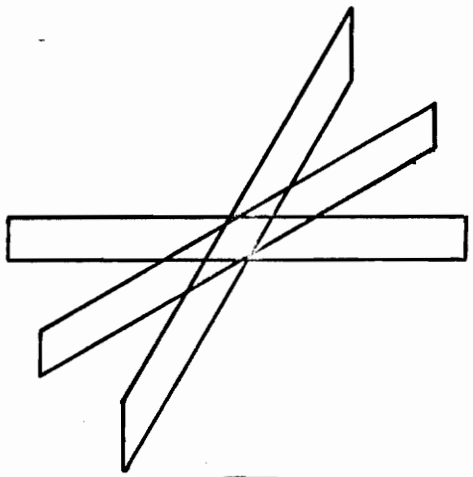	12.7	1-10
	12.7	11-19
	10.6	20
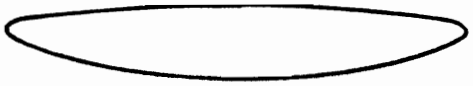	12.7	21
	12.7	22

FIG. 4 WING MODELS

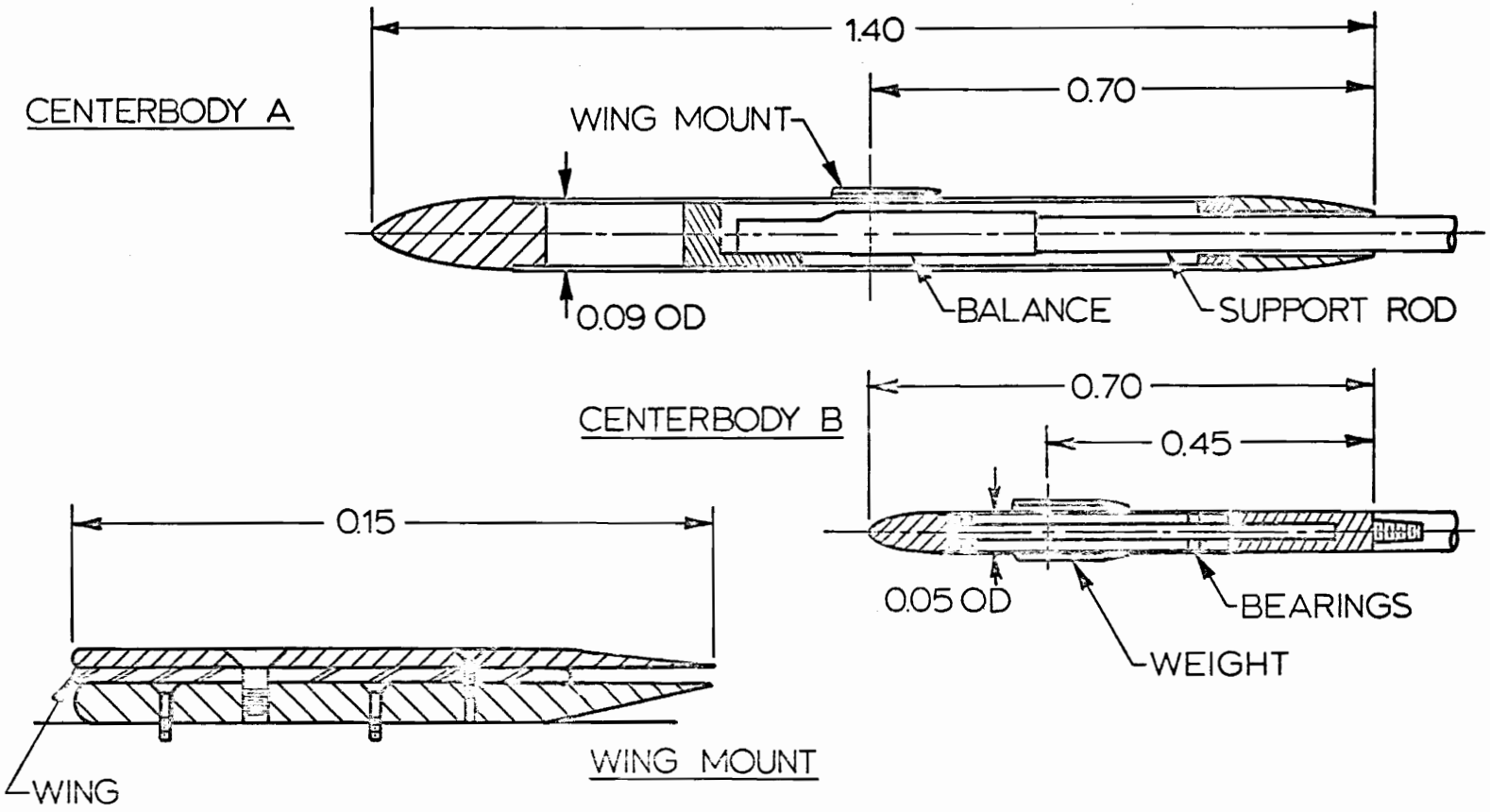

FIG. 5 CENTERBODY DESIGNS

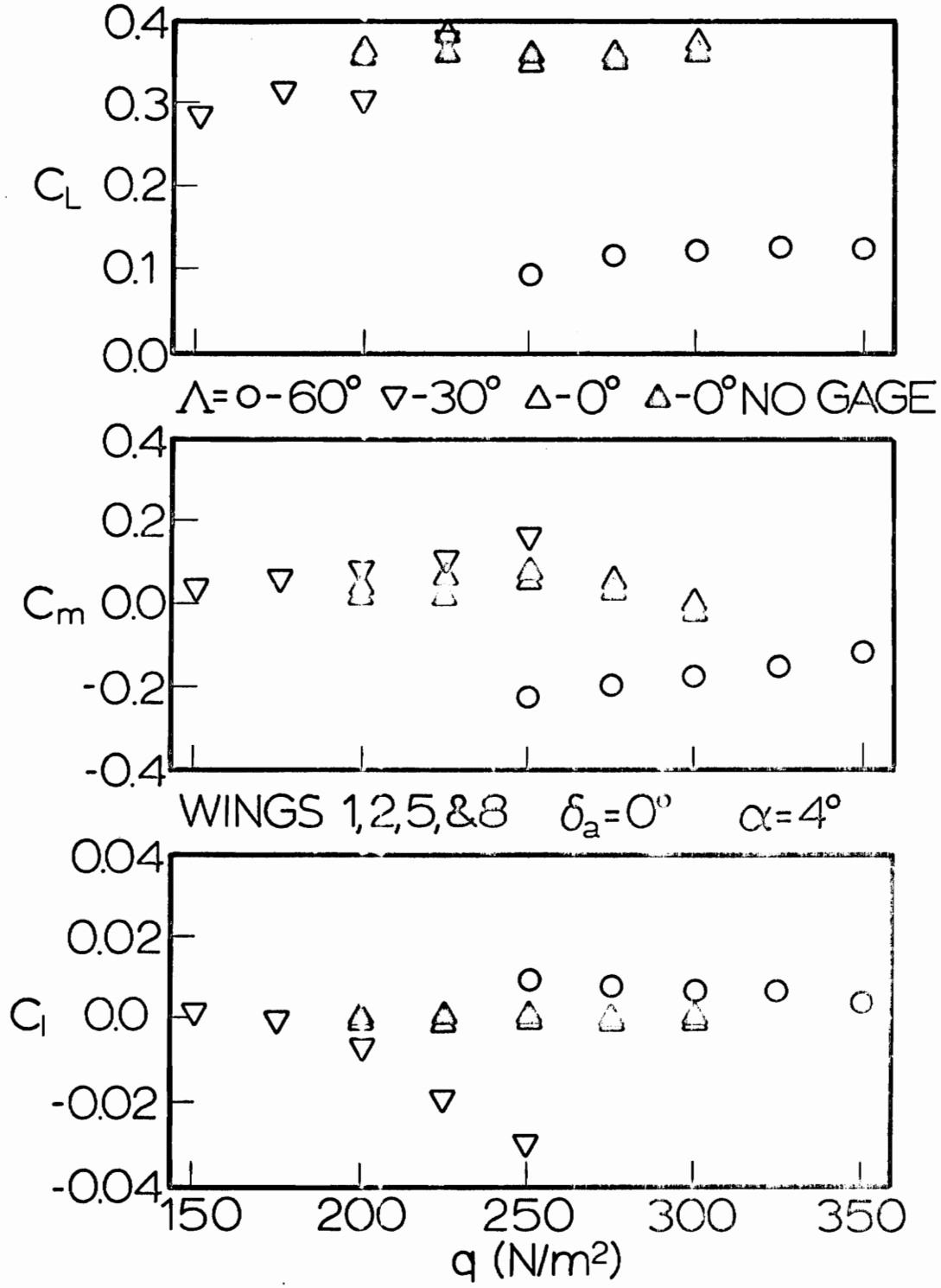

FIG.6 AERODYNAMIC DATA FOR WINGS 1,2,5,&8

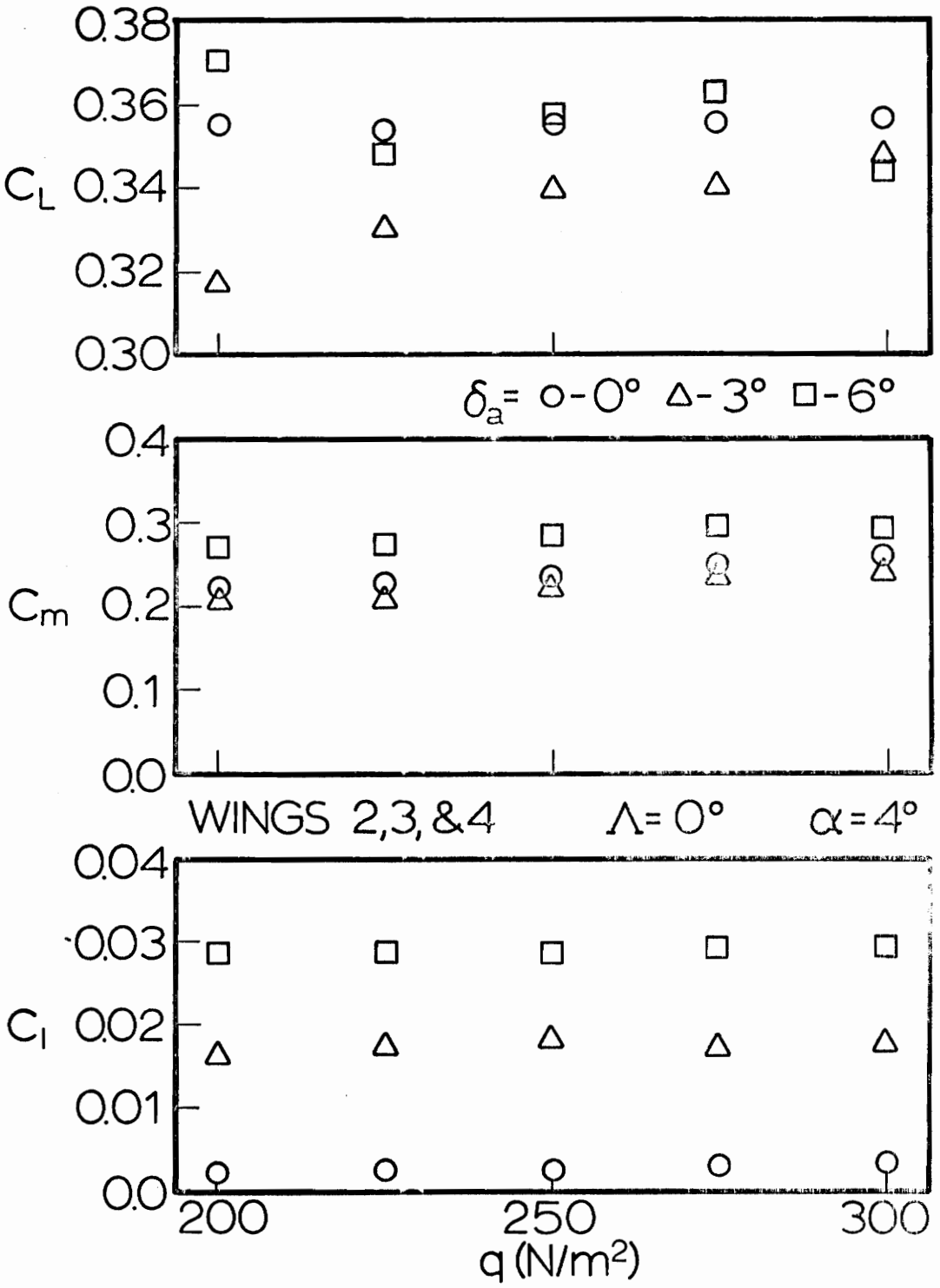

FIG. 7 AERODYNAMIC DATA FOR WINGS 2,3,&4

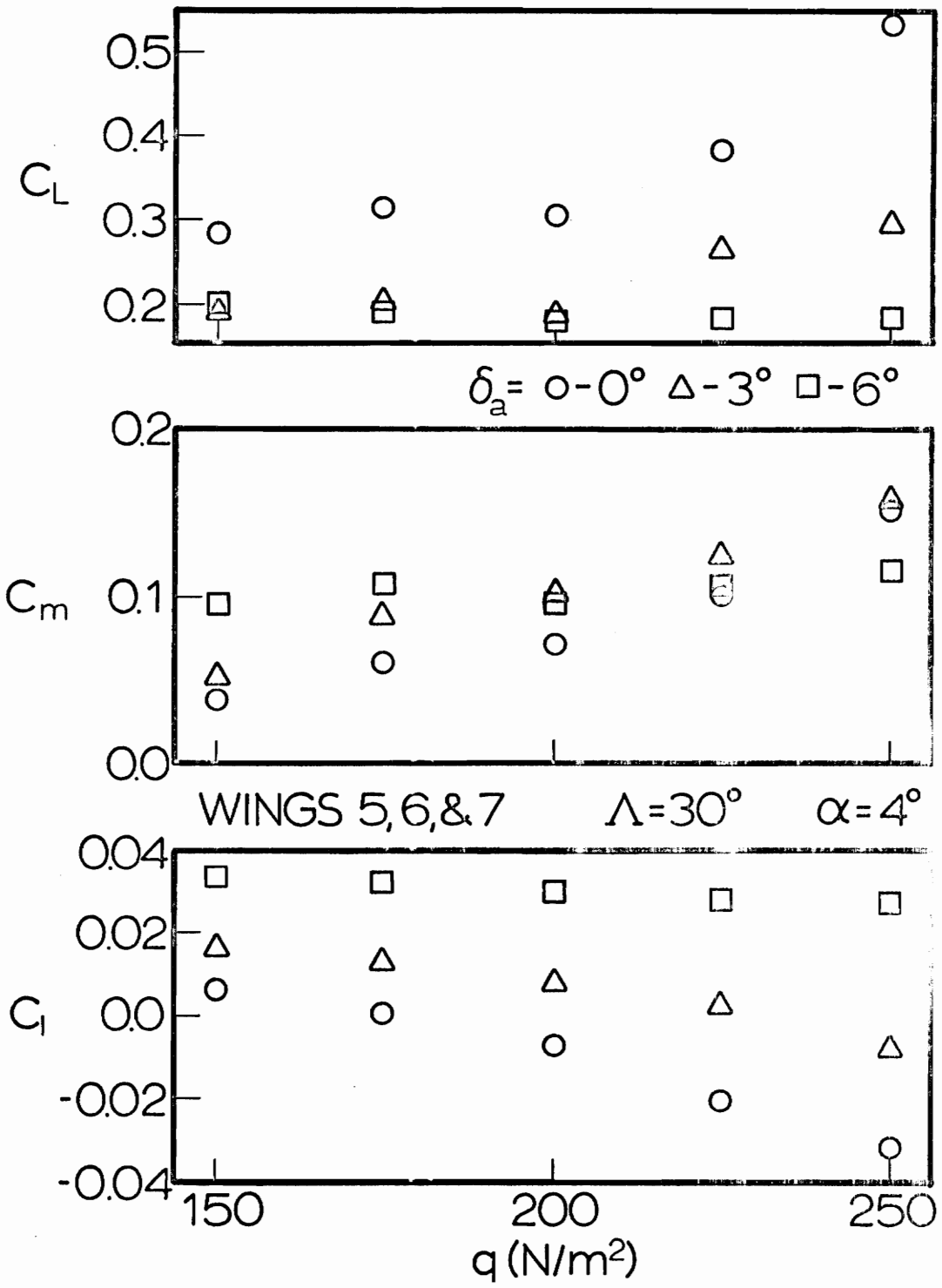

FIG. 8 AERODYNAMIC DATA FOR WINGS 5,6,&7

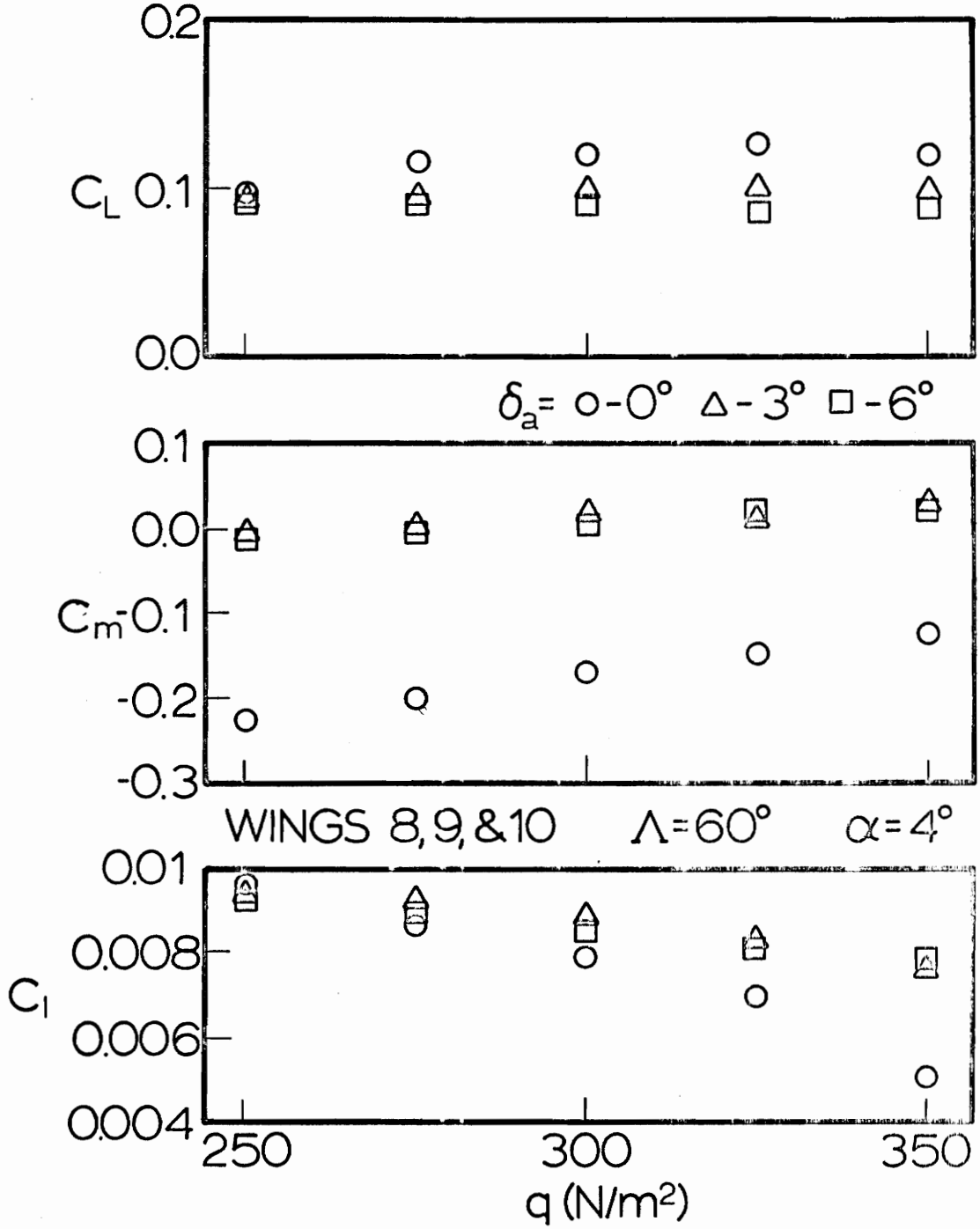

FIG.9 AERODYNAMIC DATA FOR WINGS 8,9,&10

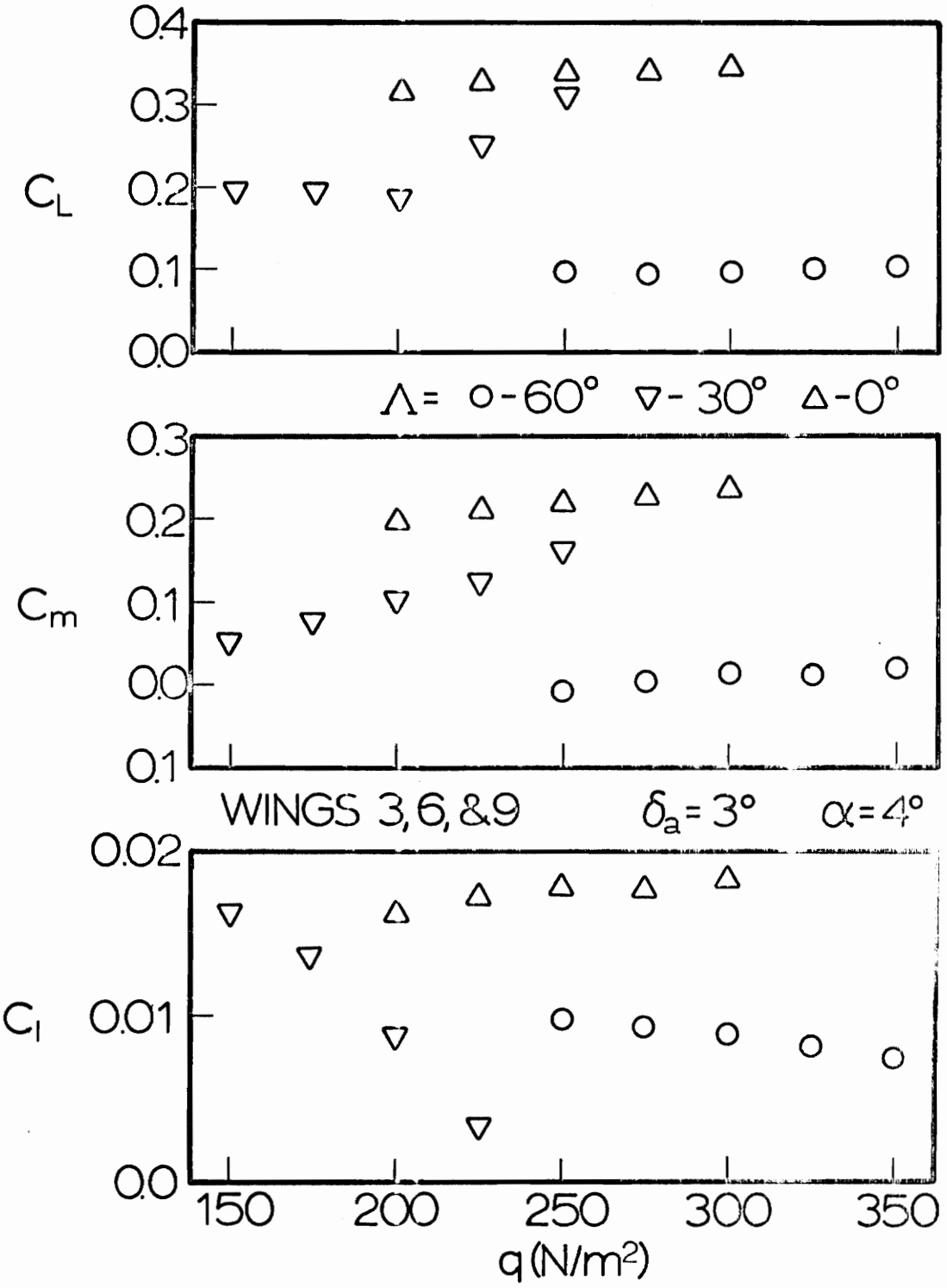

FIG. 10 AERODYNAMIC DATA FOR WINGS 3, 6, &9

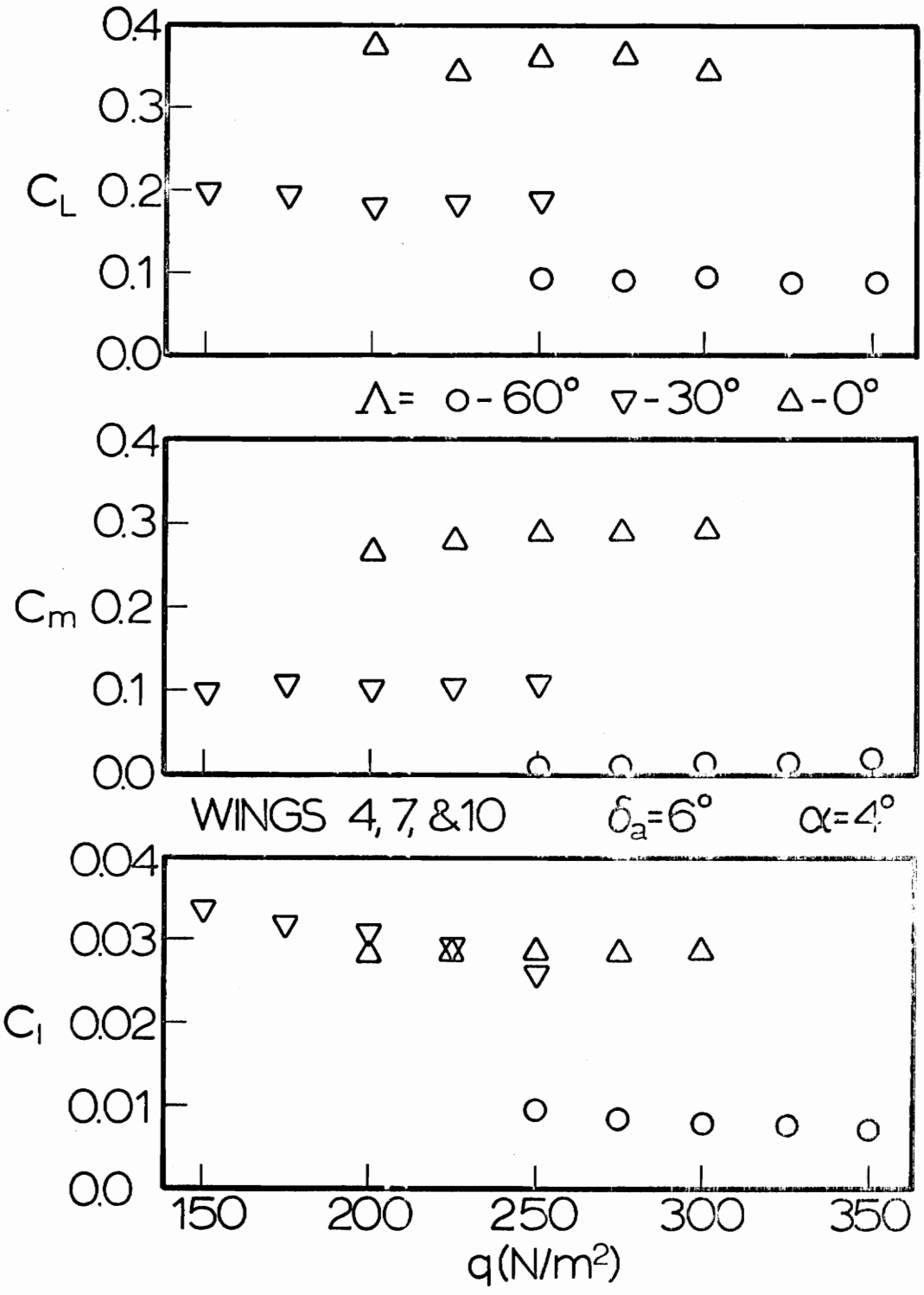

FIG.11 AERODYNAMIC DATA FOR WINGS 4, 7, &10

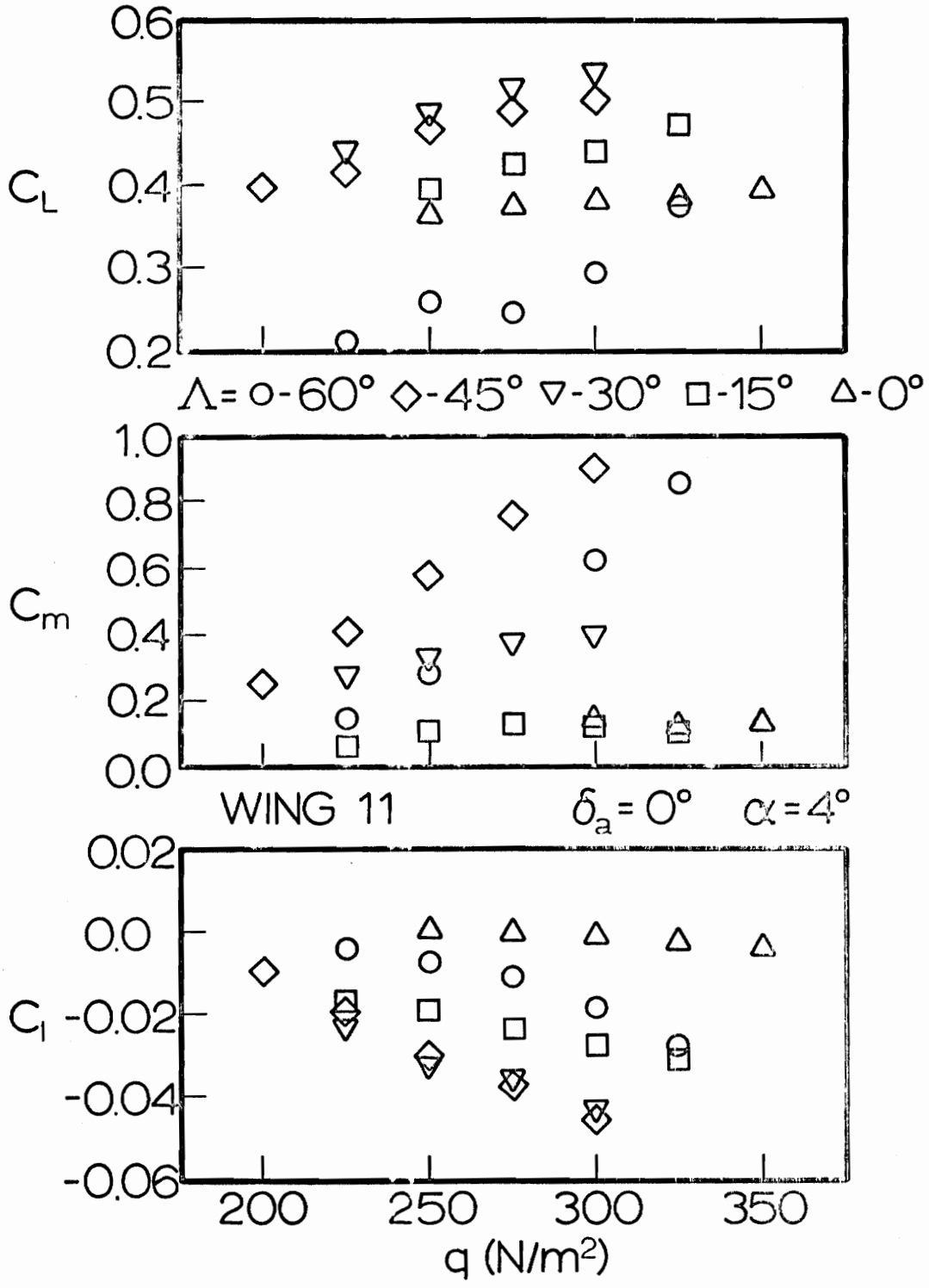

FIG. 12 AERODYNAMIC DATA FOR WING 11

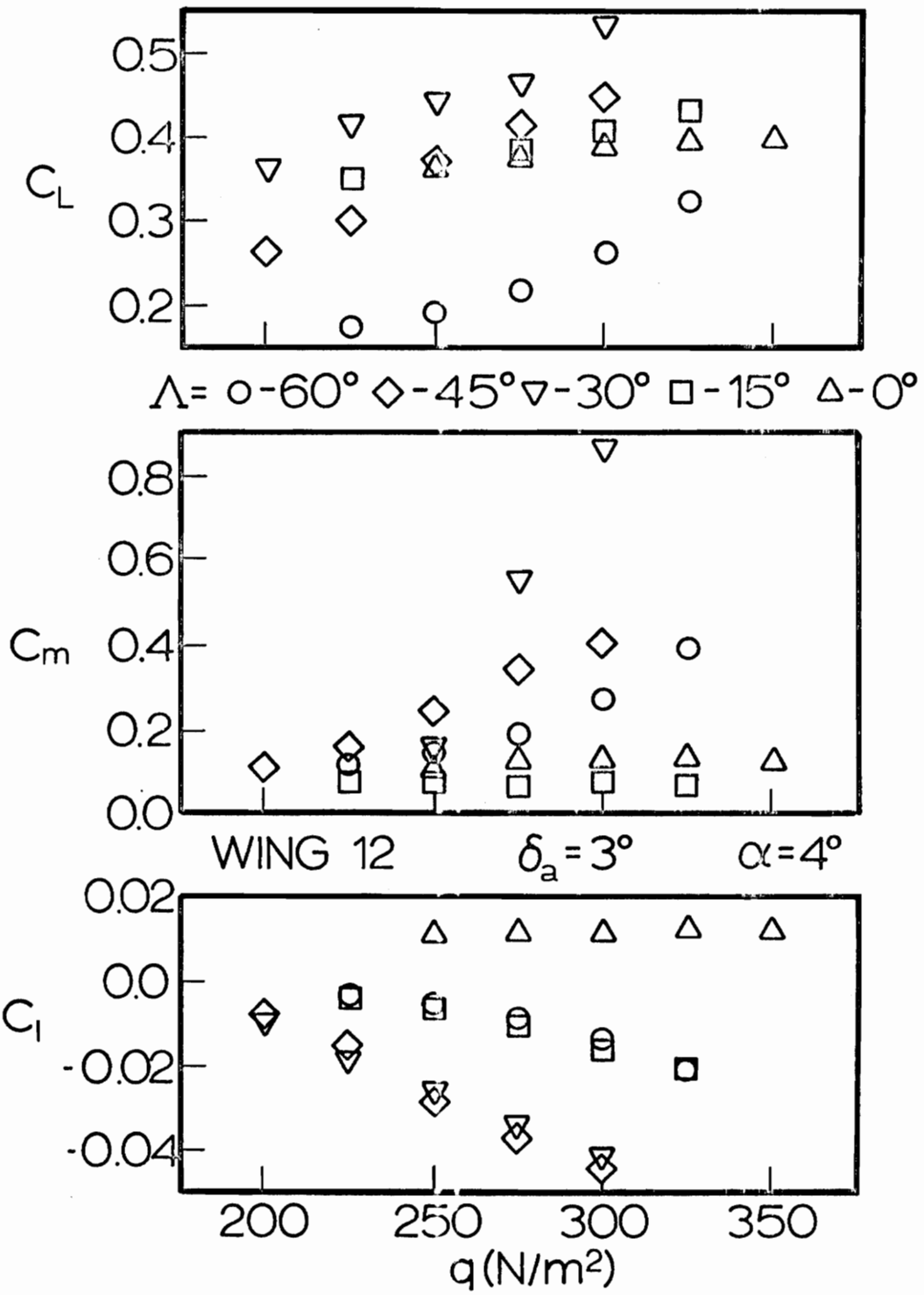

FIG. 13 AERODYNAMIC DATA FOR WING 12

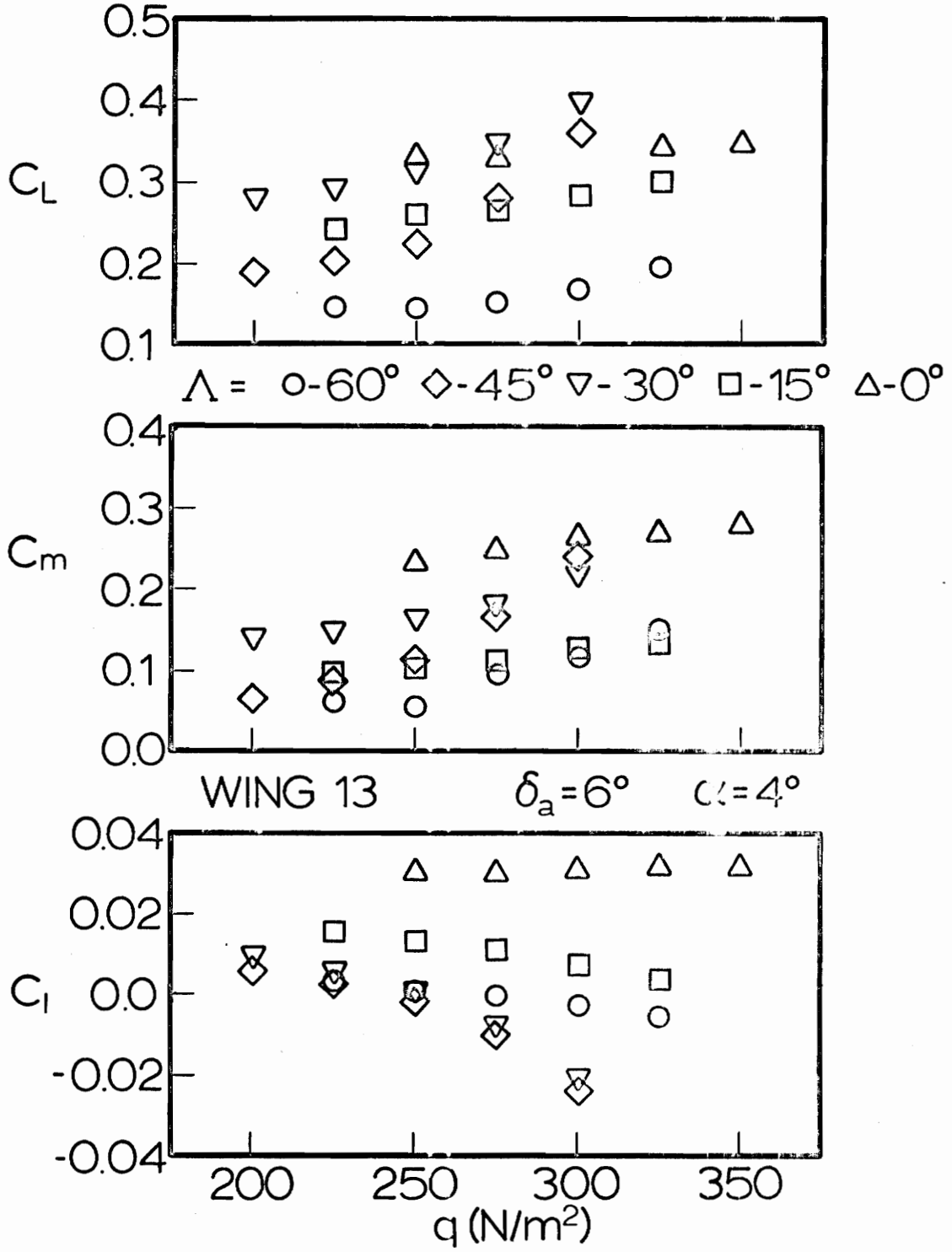

FIG. 14 AERODYNAMIC DATA FOR WING 13

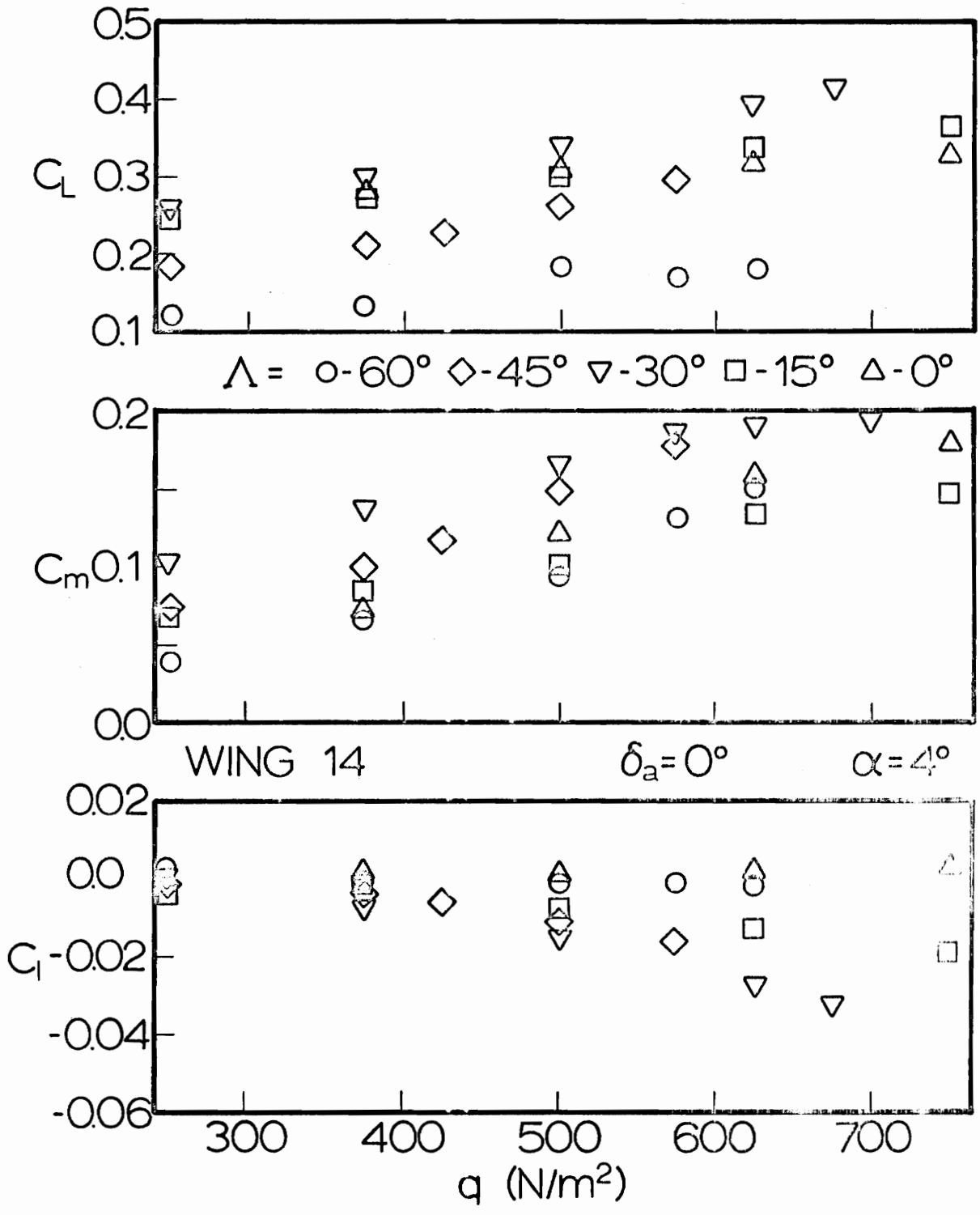

FIG. 15 AERODYNAMIC DATA FOR WING 14

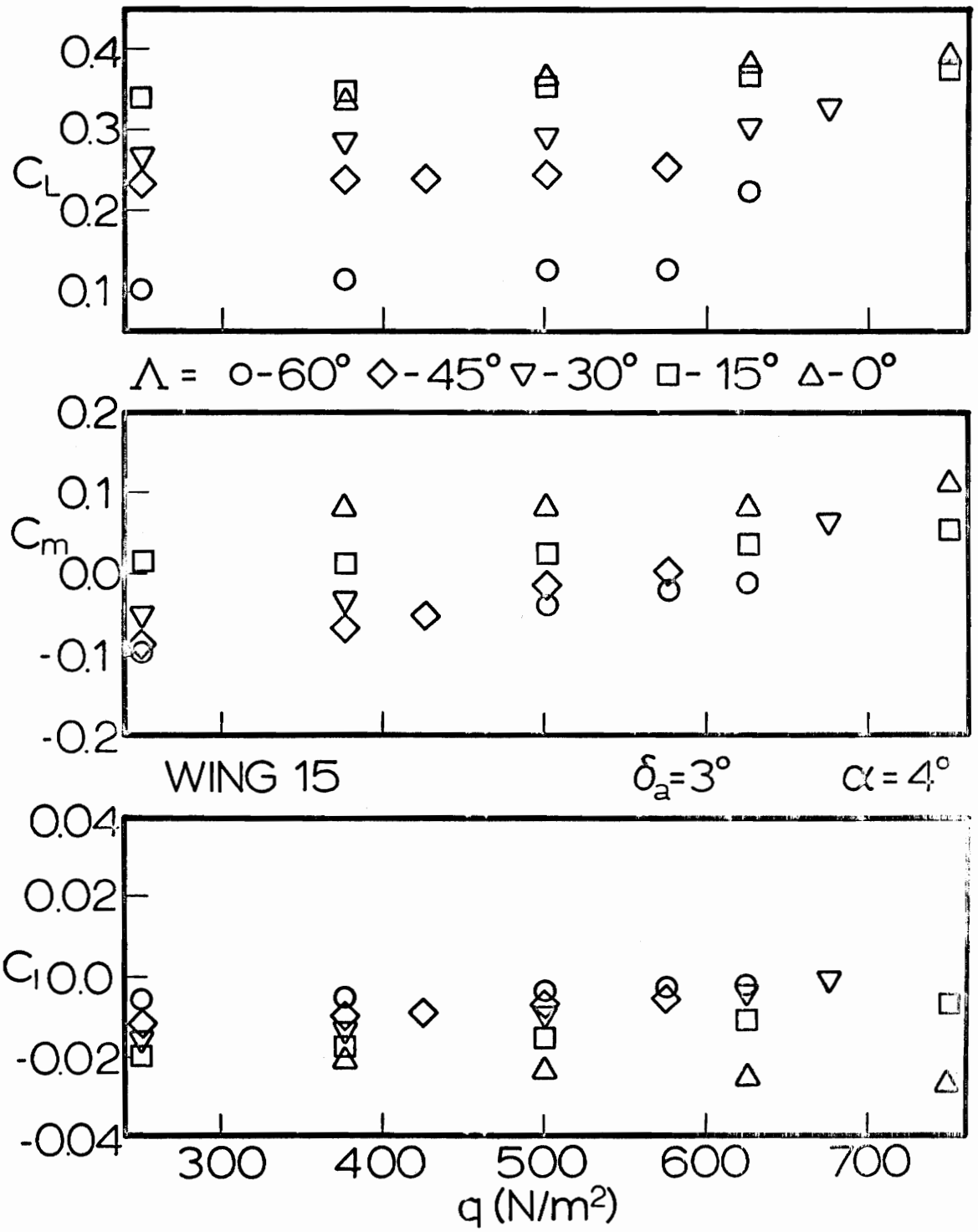

FIG. 16 AERODYNAMIC DATA FOR WING 15

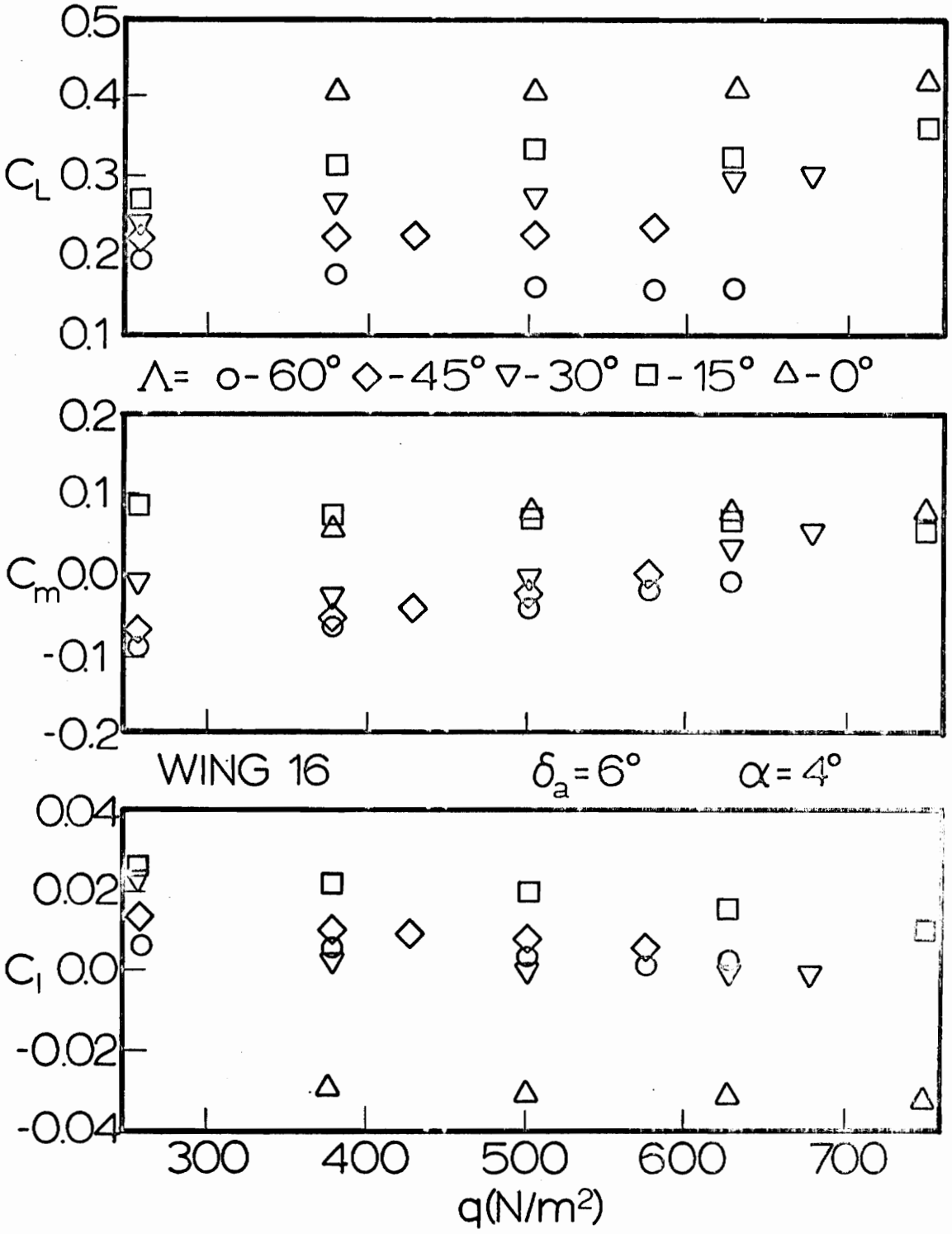

FIG. 17 AERODYNAMIC DATA FOR WING 16

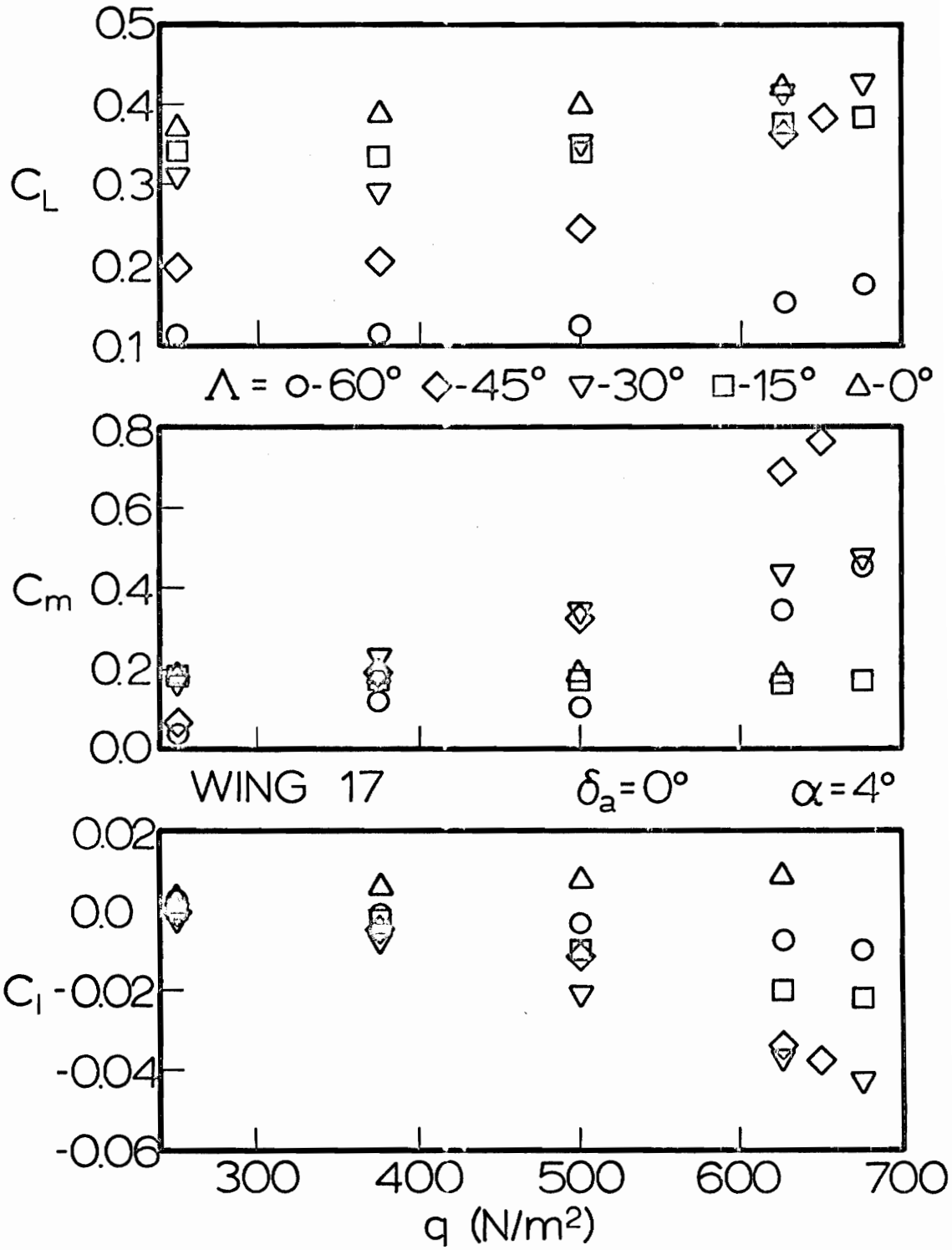

FIG. 18 AERODYNAMIC DATA FOR WING 17

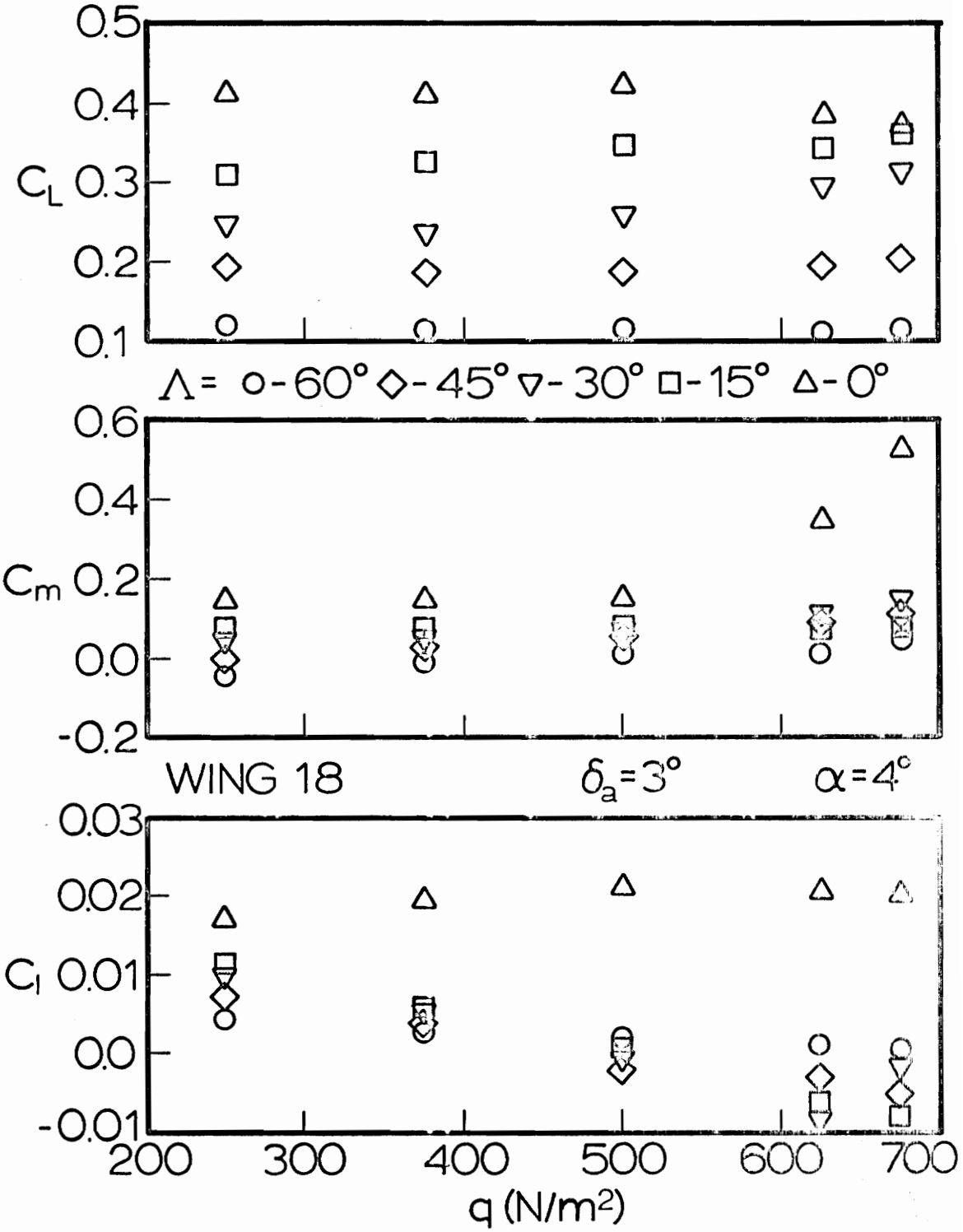

FIG. 19 AERODYNAMIC DATA FOR WING 18

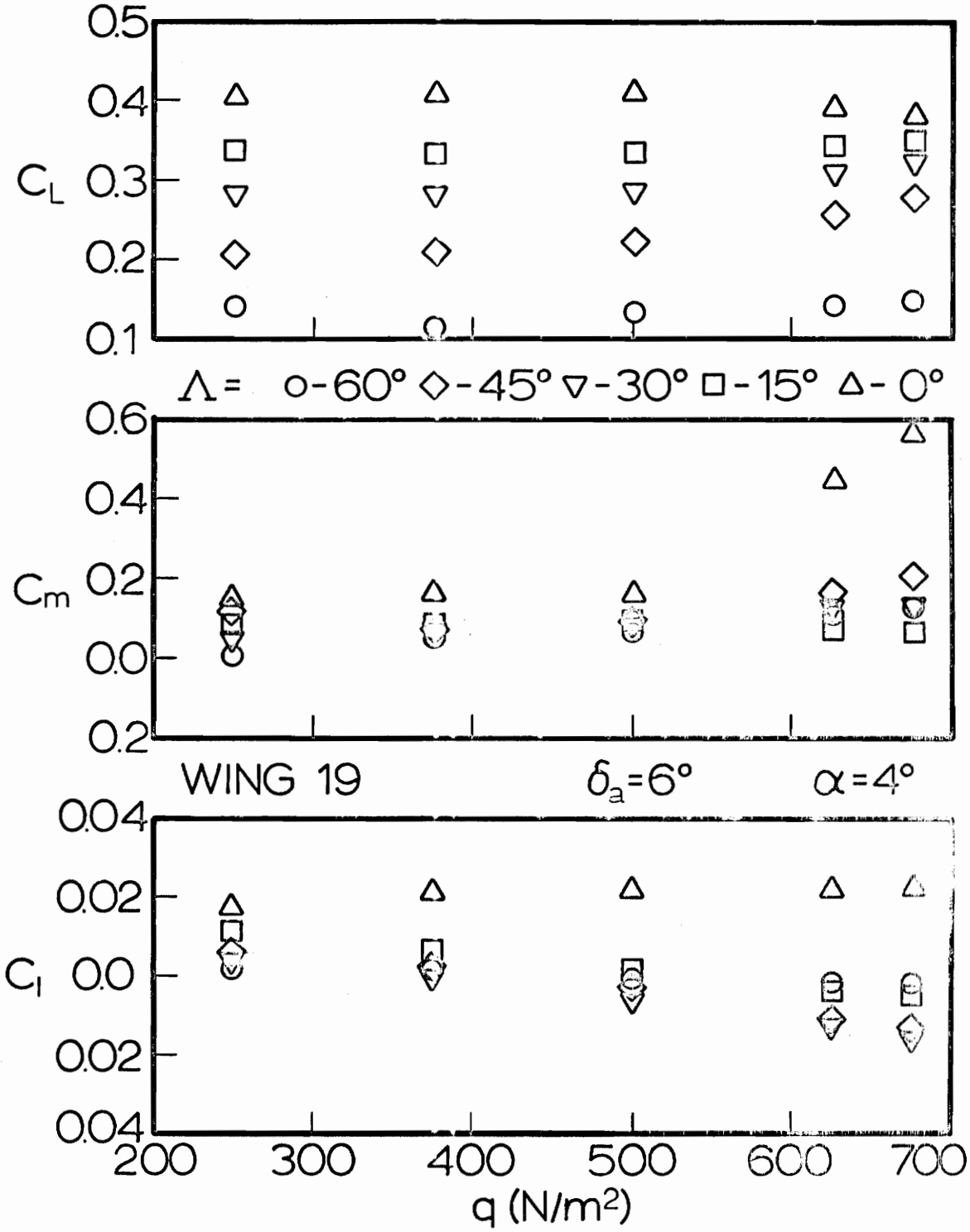

FIG. 20 AERODYNAMIC DATA FOR WING 19

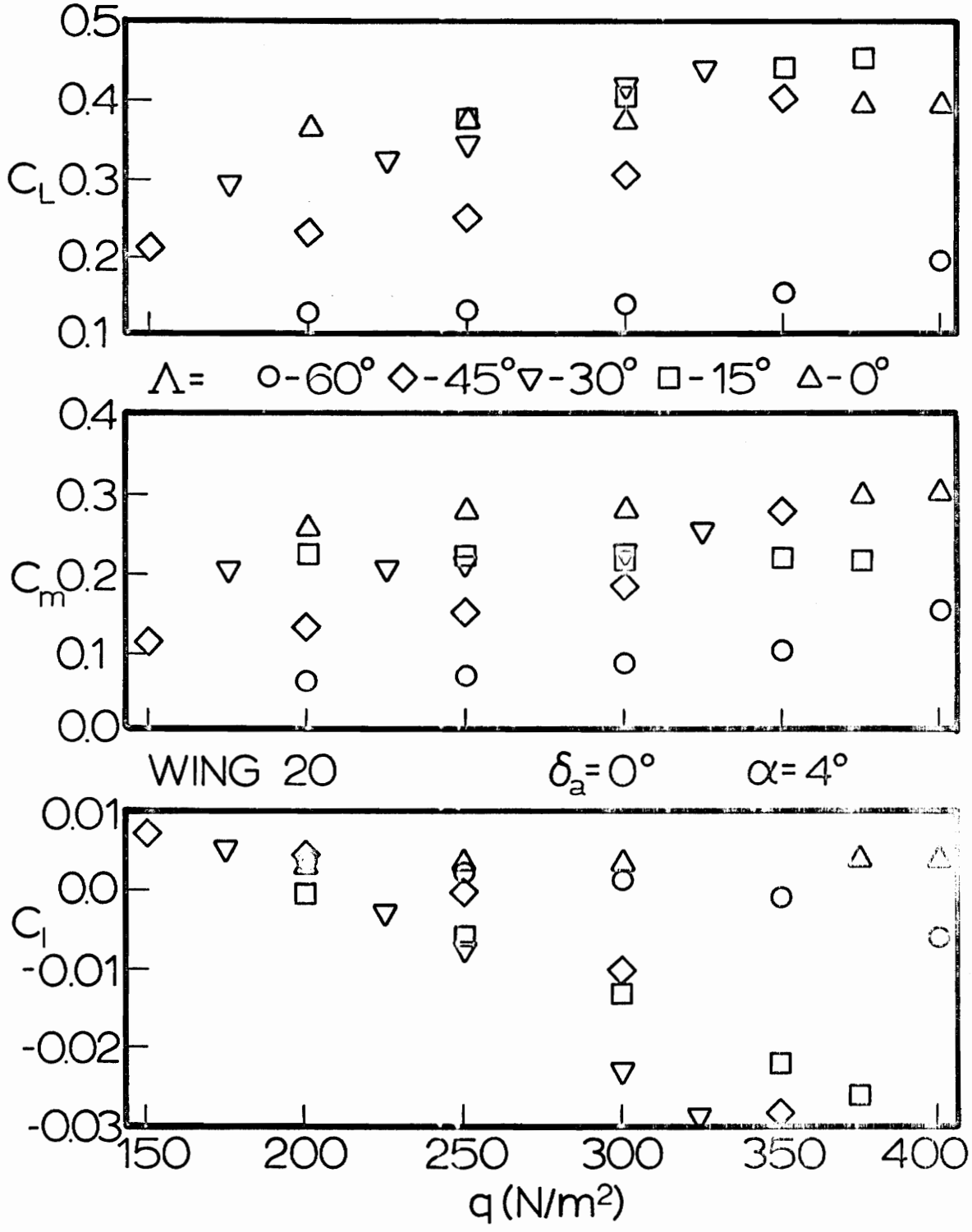

FIG. 21 AERODYNAMIC DATA FOR WING 20

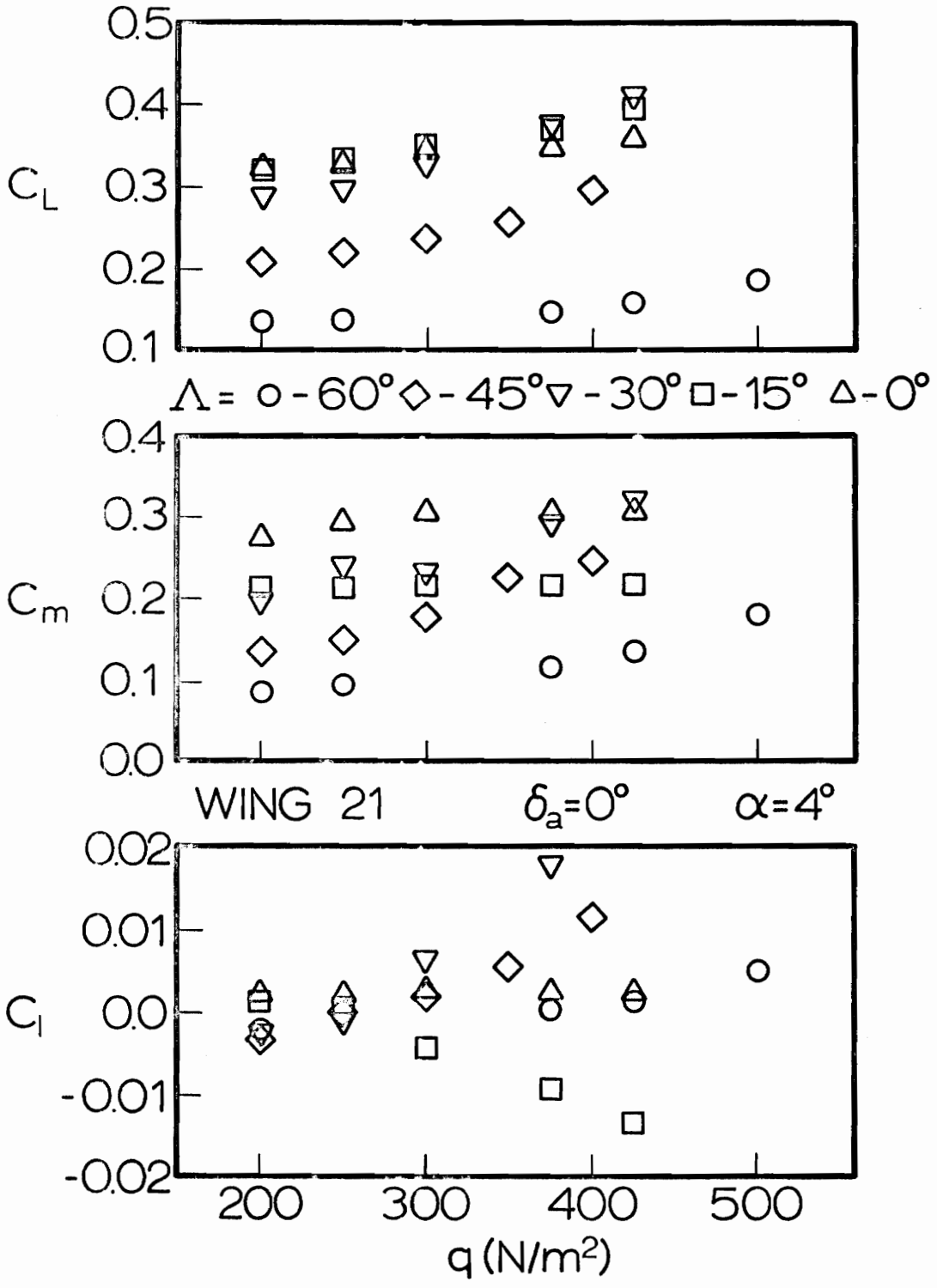

FIG. 22 AERODYNAMIC DATA FOR WING 21

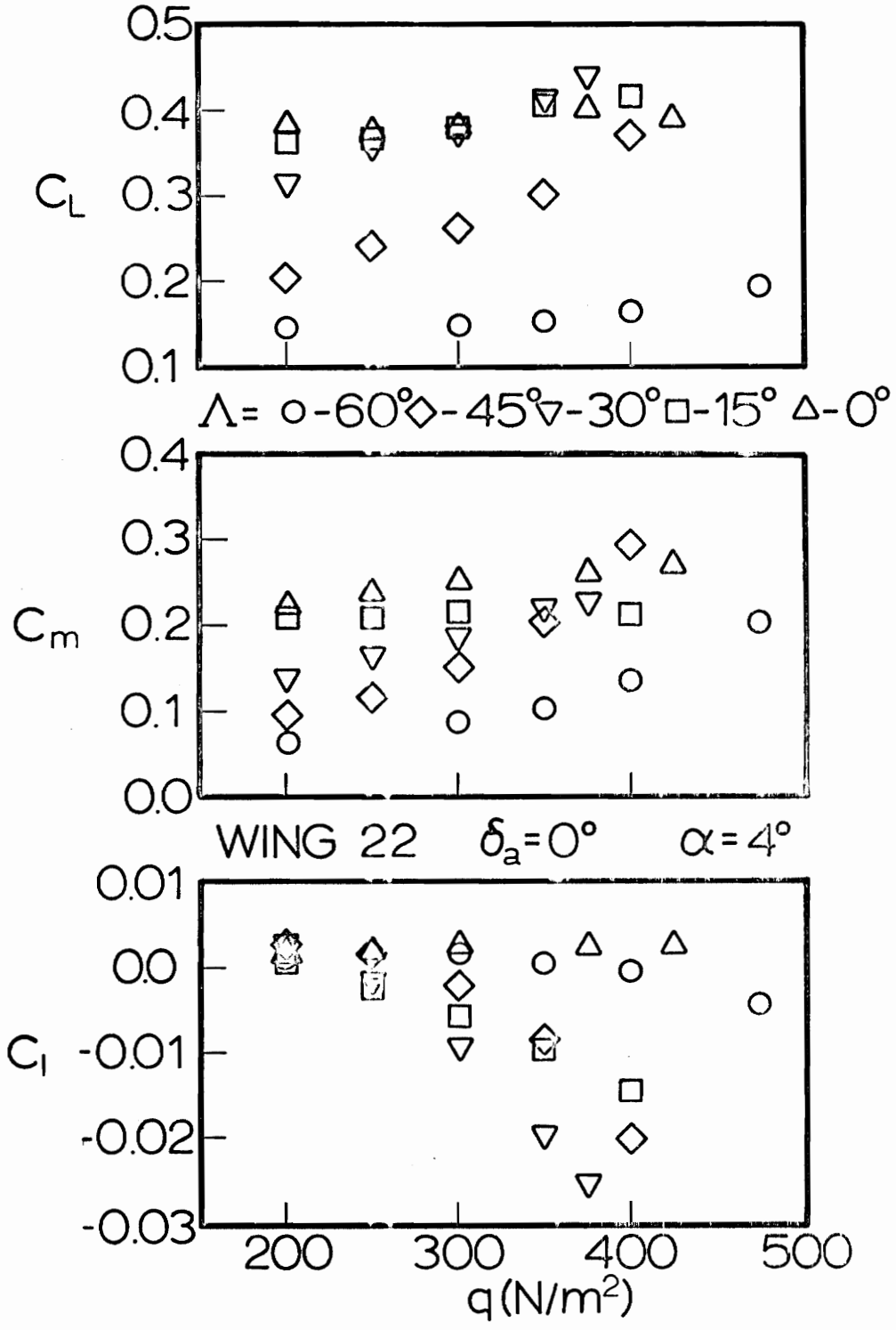

FIG. 23 AERODYNAMIC DATA FOR WING 22

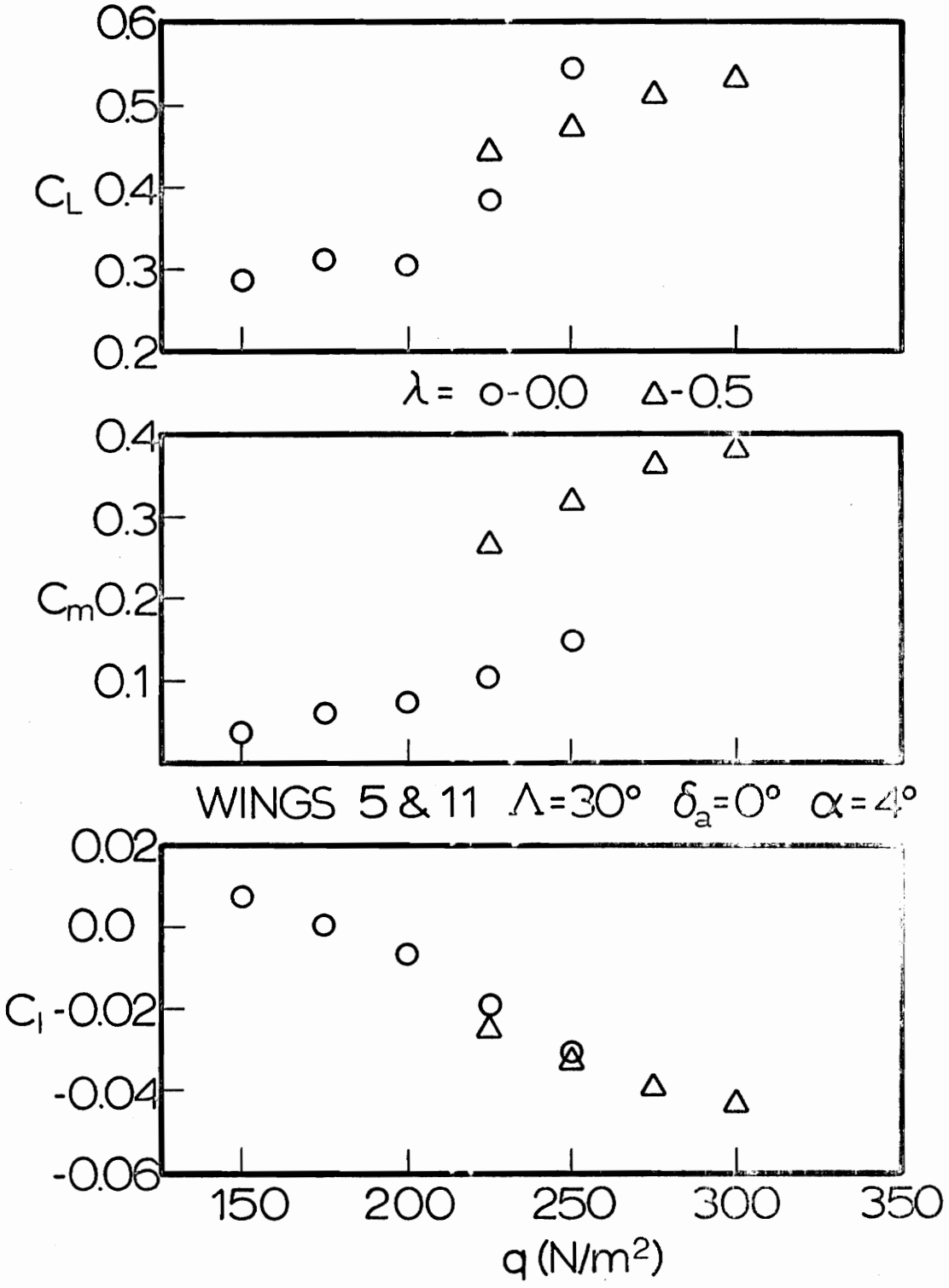

FIG. 24 TAPER RATIO TRENDS

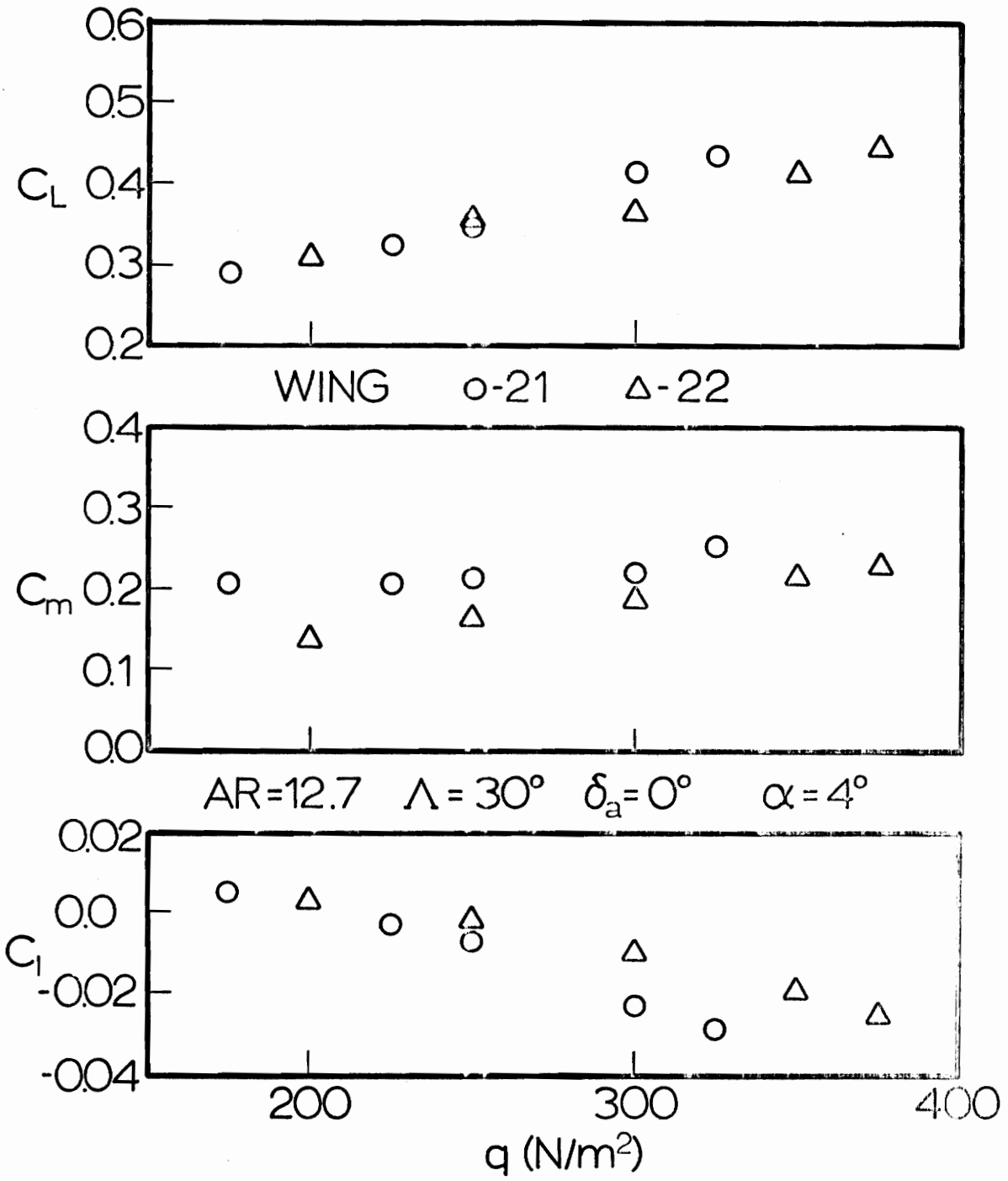

FIG. 25 PLANFORM TRENDS

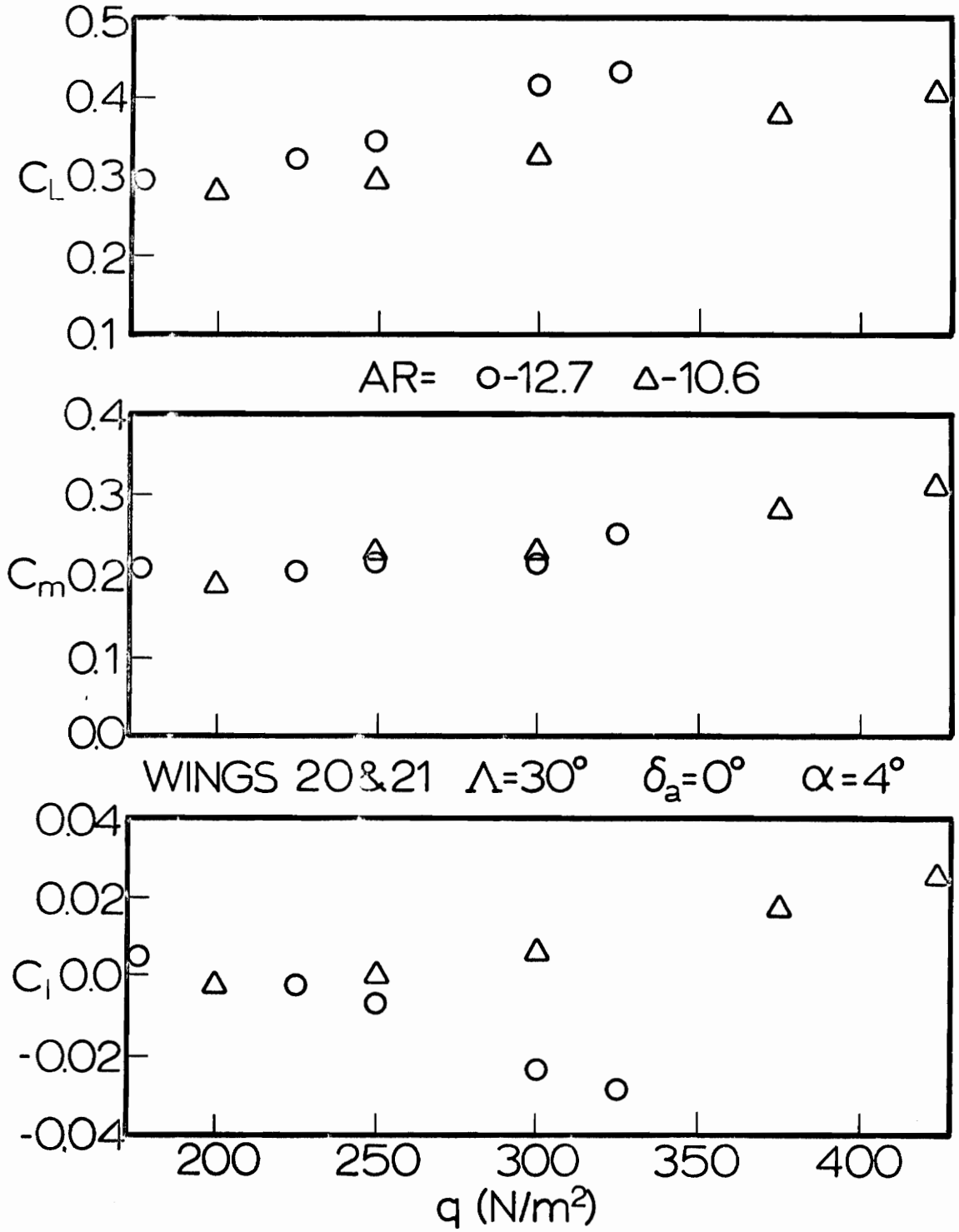

FIG.26 ASPECT RATIO TRENDS

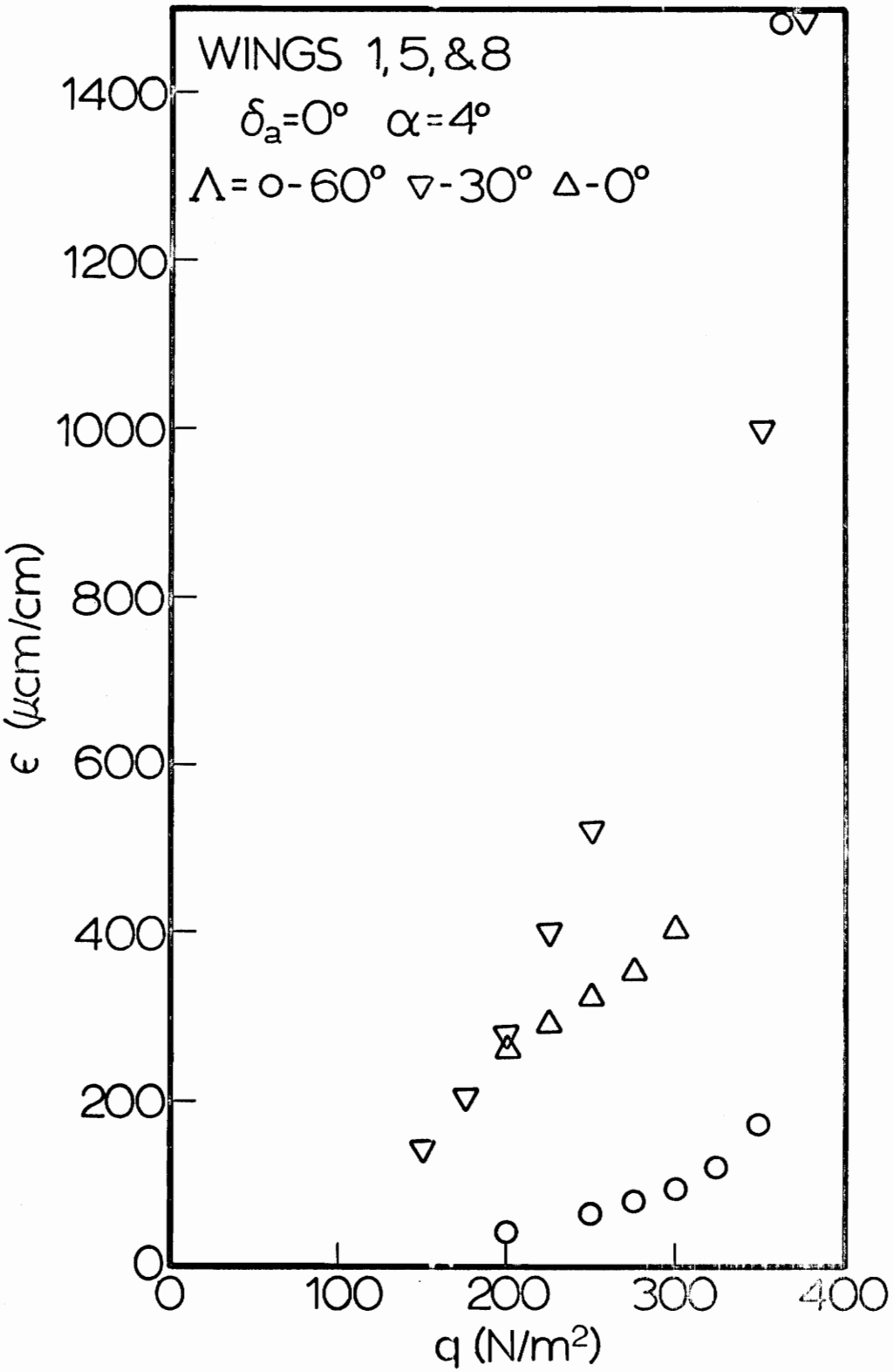

FIG. 27 STRAIN IN WINGS 1, 5, & 8

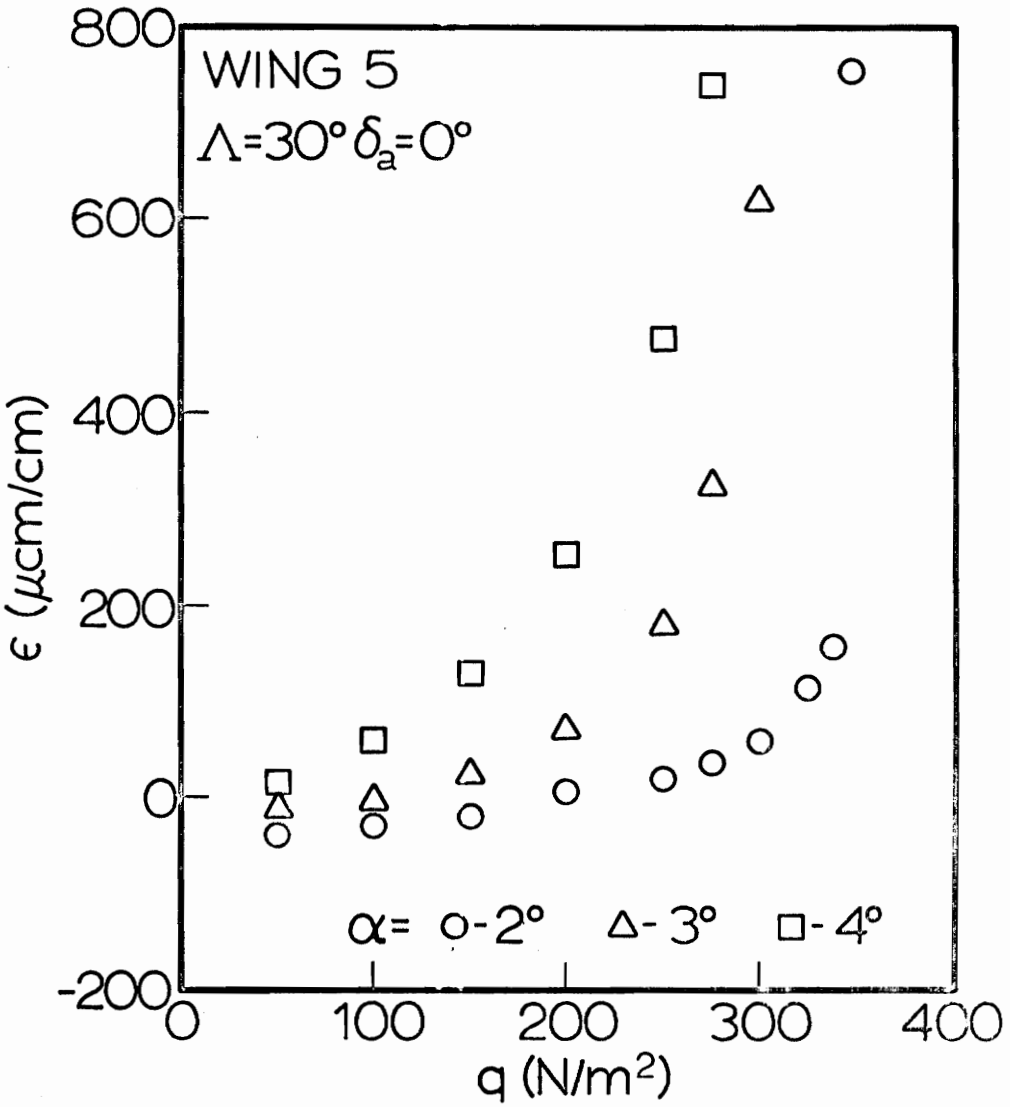

FIG. 28 STRAIN AT VARIOUS ANGLES OF ATTACK

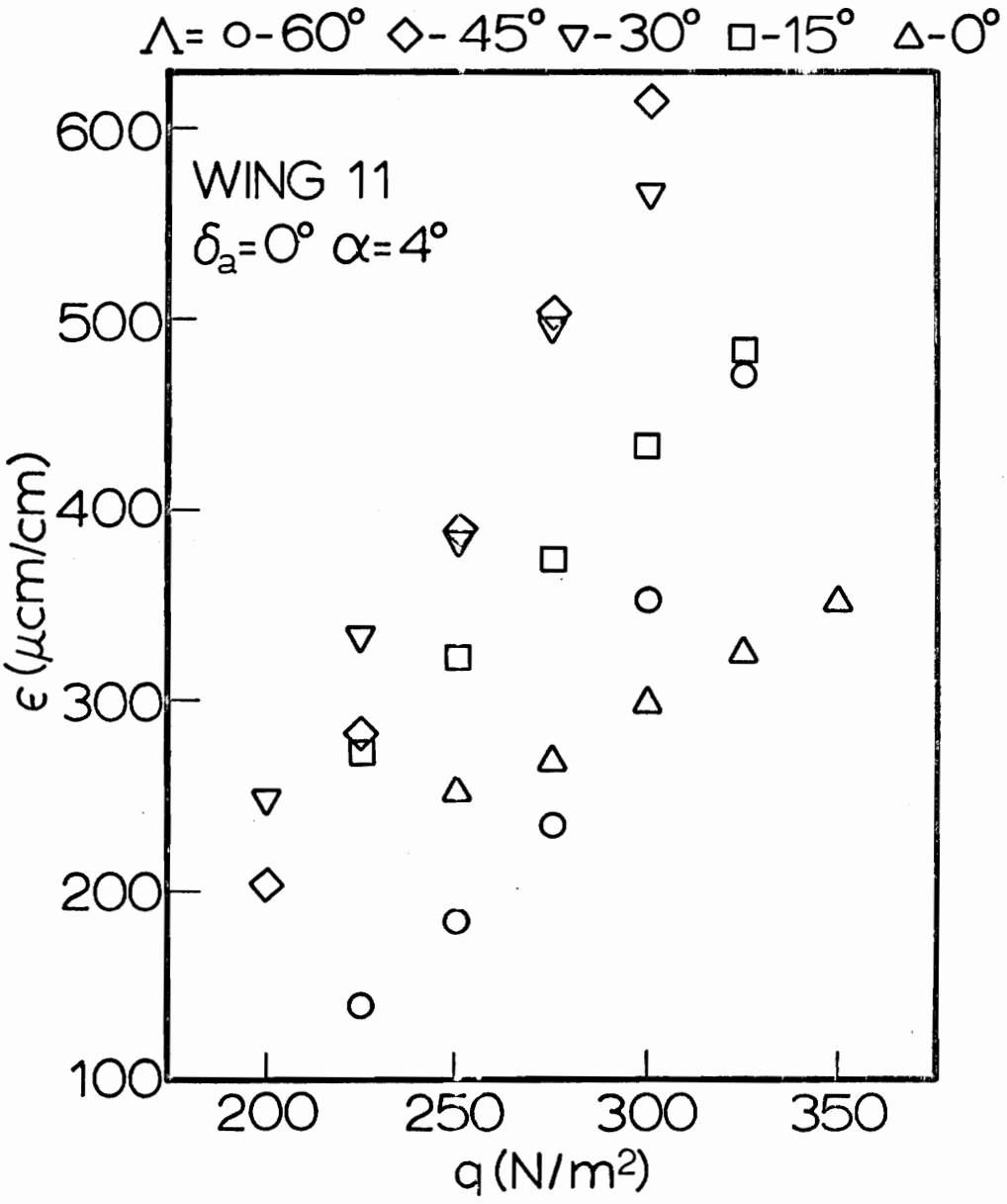

FIG. 29 STRAIN IN WING 11

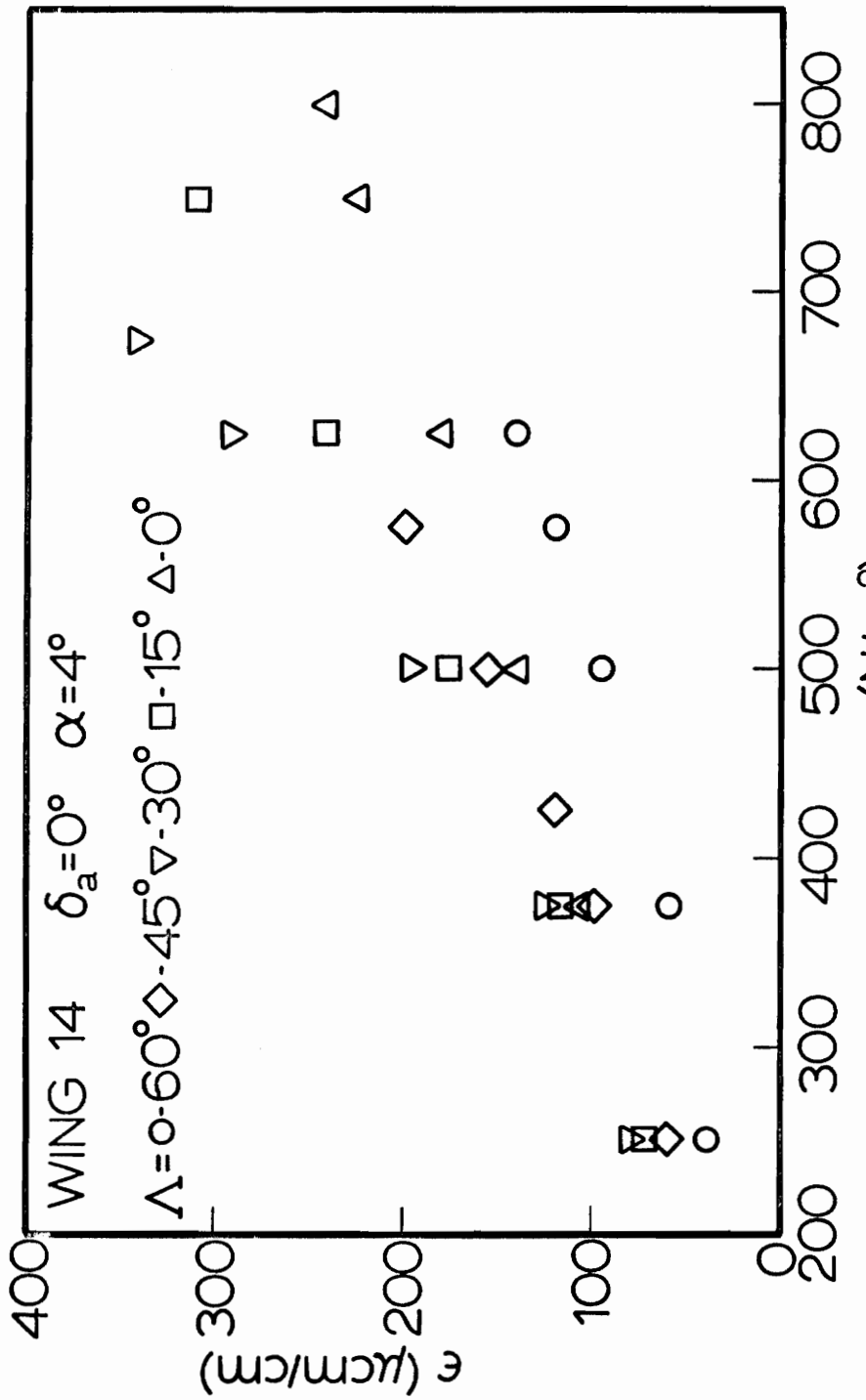

FIG. 30 STRAIN IN WING 14

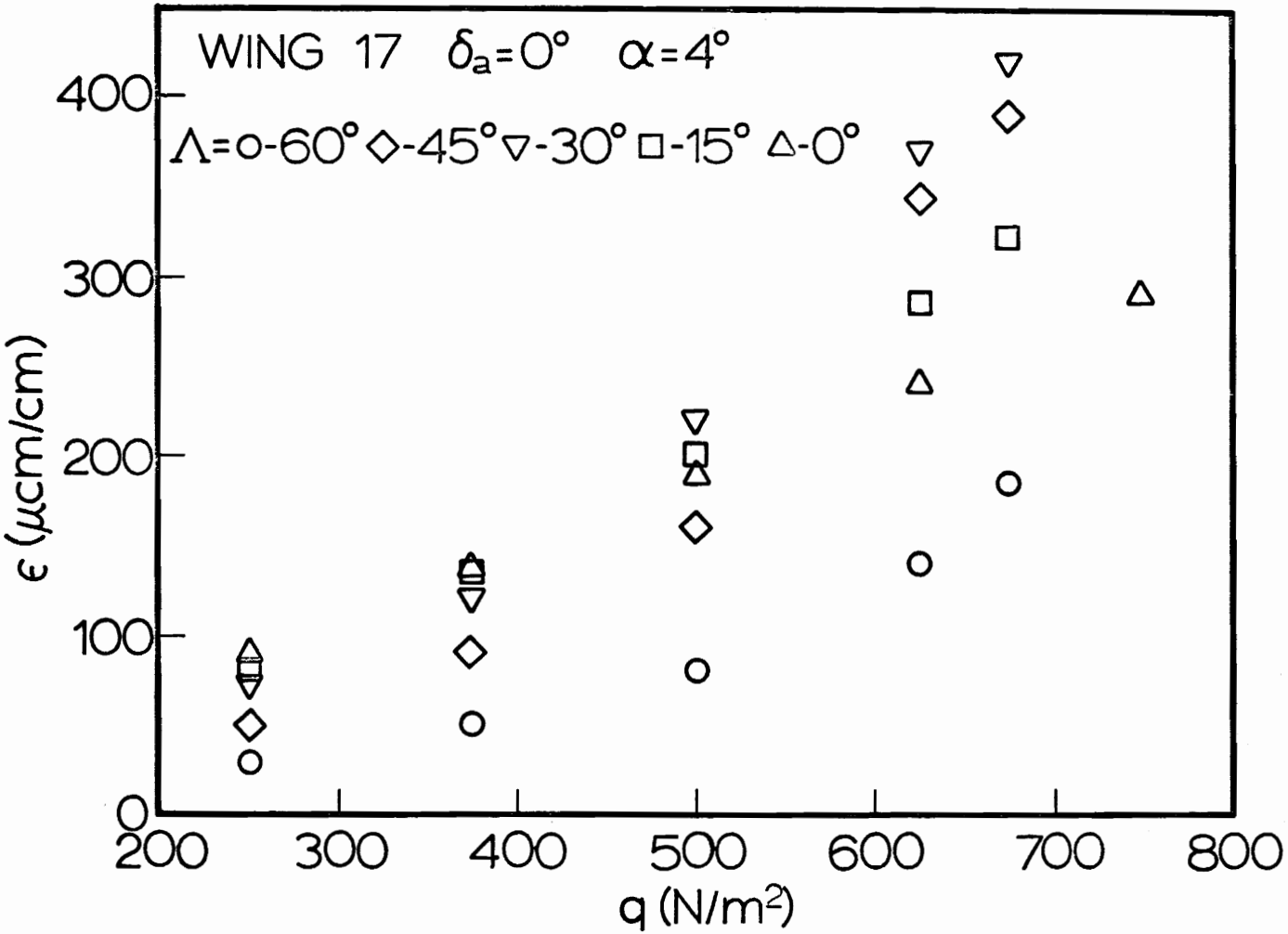

FIG. 31 STRAIN IN WING 17

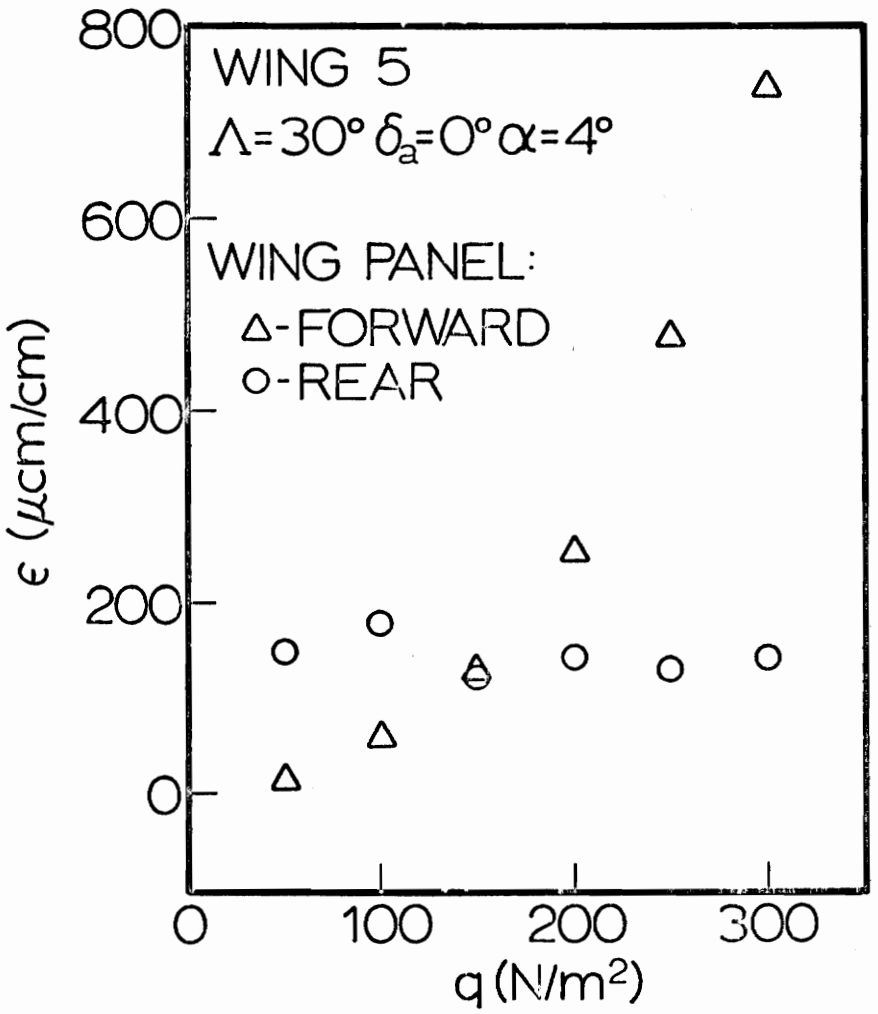

FIG. 32 STRAIN IN SWEPTFORWARD AND SWEPTBACK PANELS

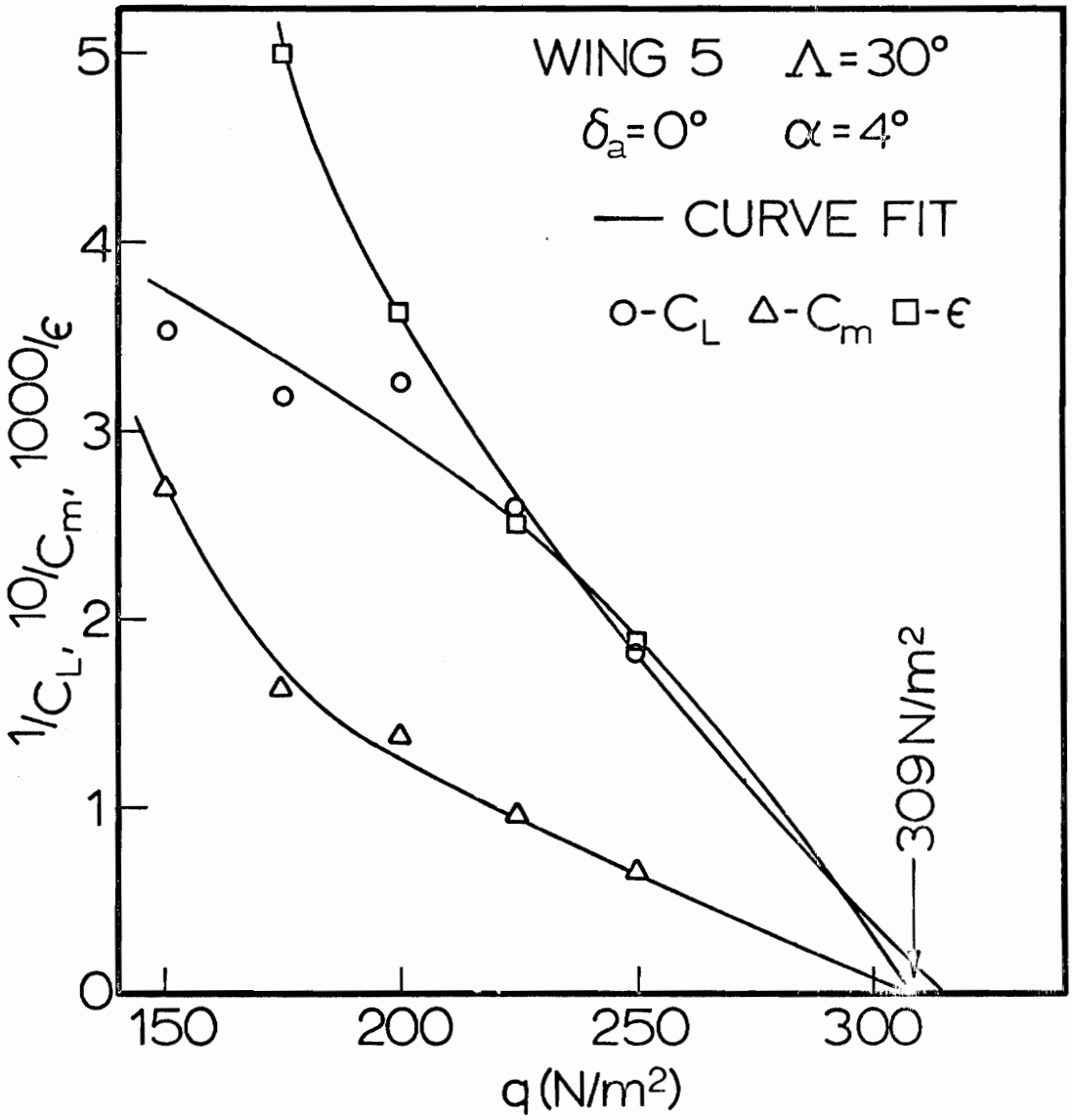

FIG. 33 DETERMINATION OF DIVERGENCE VELOCITY

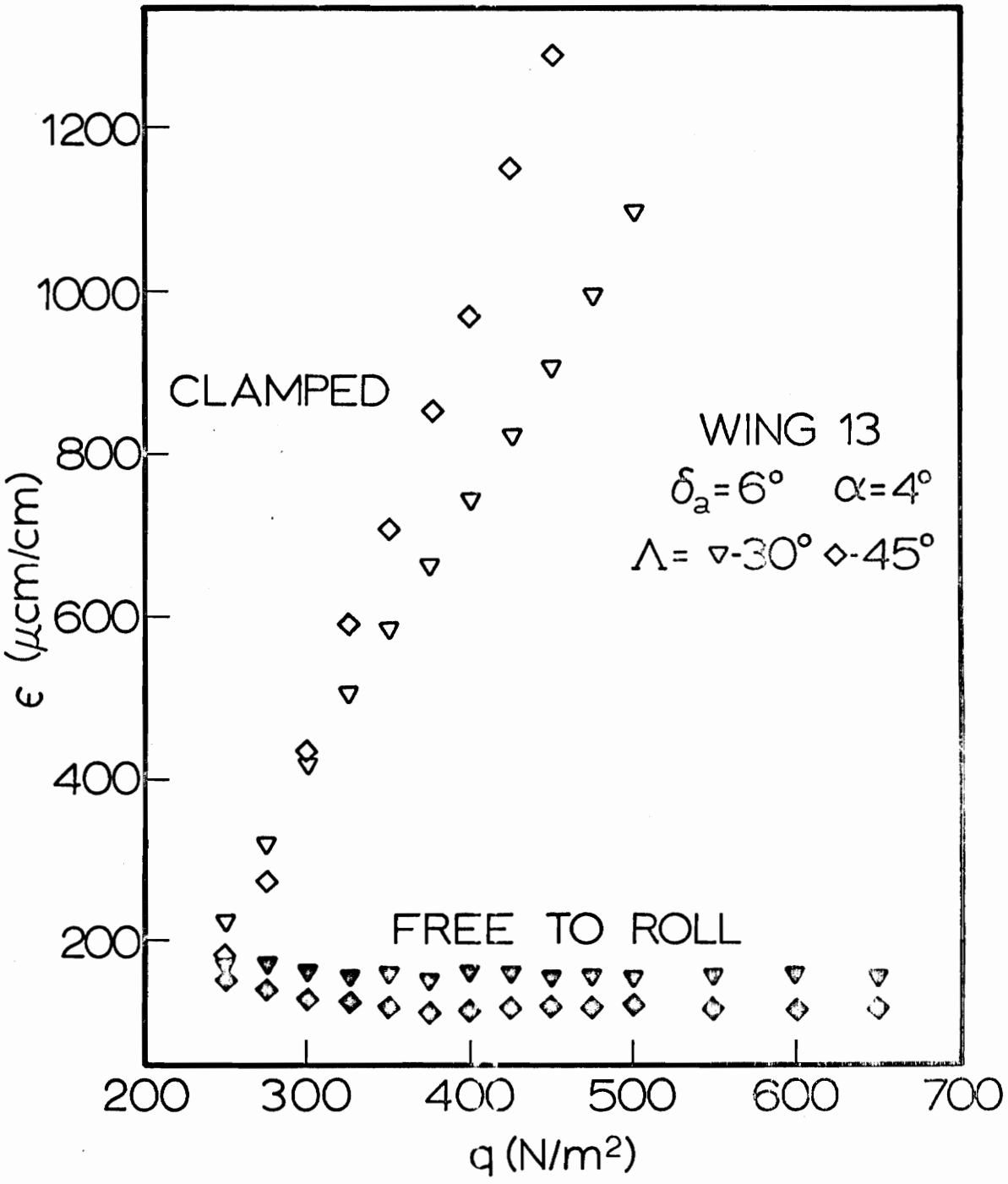

FIG. 34 EFFECT OF ROLL CONSTRAINT ON WING STRAIN

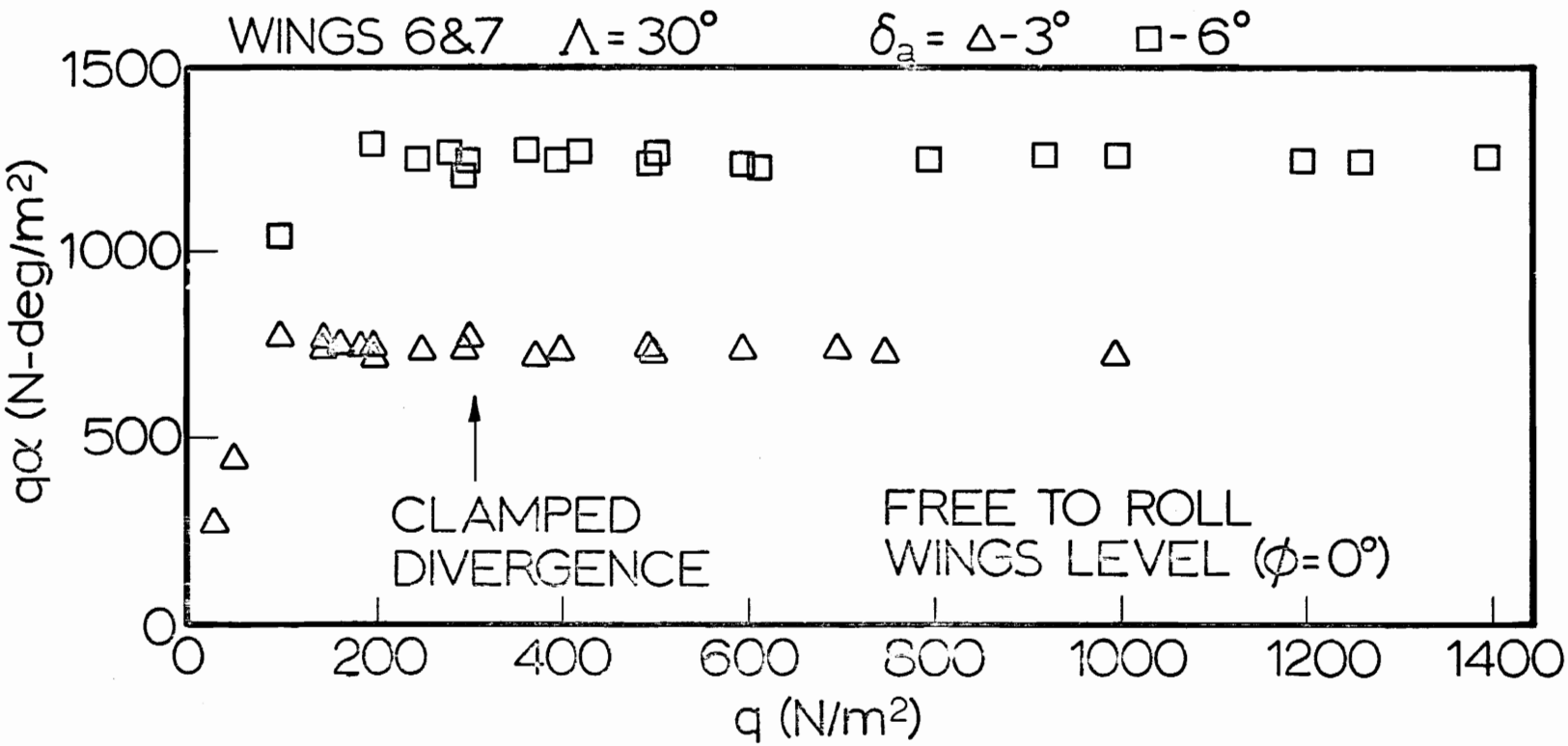

FIG 35 WING LOADING DATA

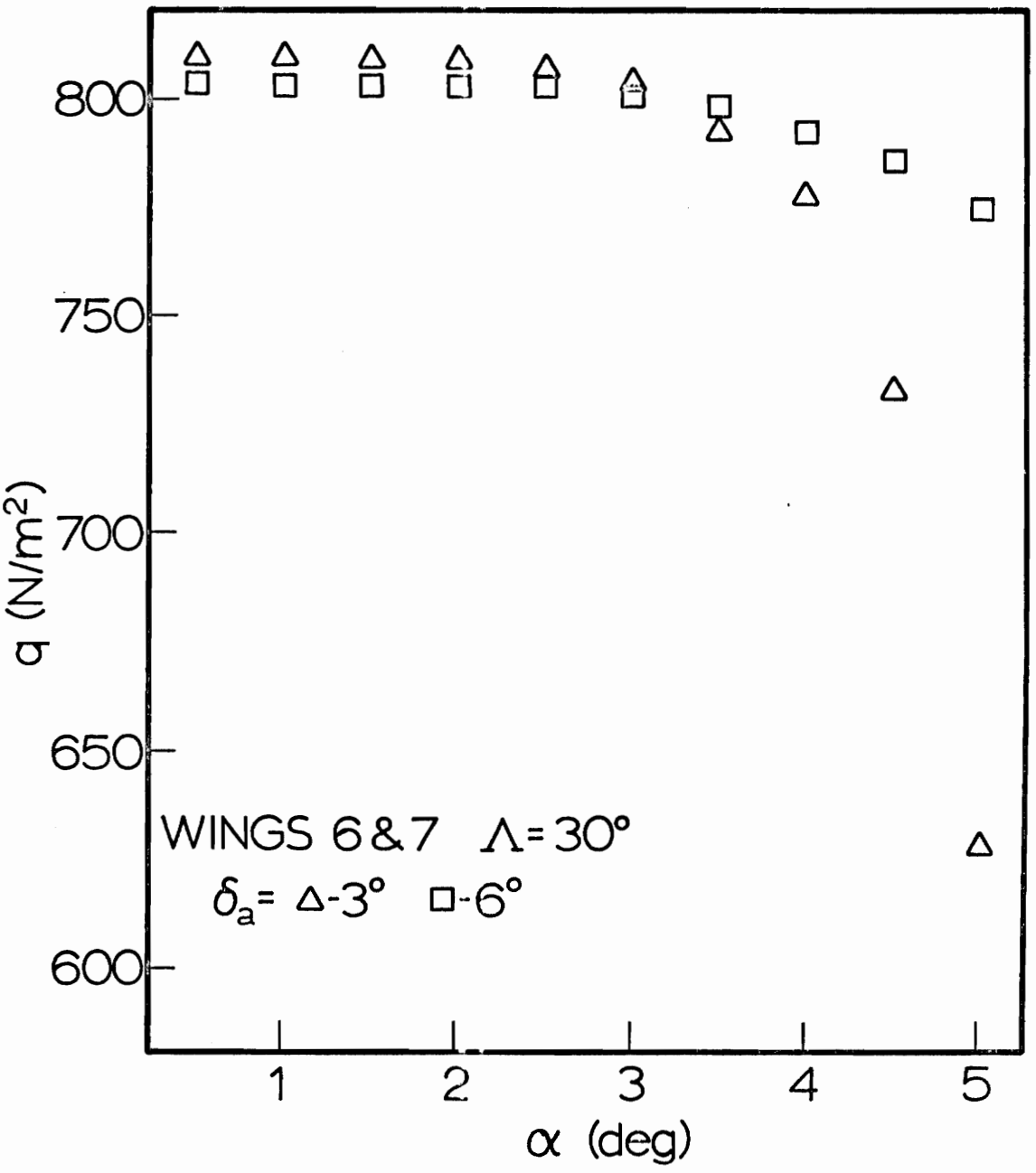

FIG. 36 FLUTTER DYNAMIC PRESSURES

APPENDIX A

THE VIRGINIA TECH STABILITY WIND TUNNEL

The Virginia Tech Stability Wind Tunnel was designed and built at the N.A.S.A. Langley Research Center in the early 1940's. It was intended to test small models and obtain lateral stability data. In 1958 the tunnel was disassembled and shipped to VPI&SU where it has been in operation since.

The tunnel has two test sections; each 7.02 m (23.0 ft) long. One is 1.83 m (6.0 ft) square and is used for conventional testing; the other is 1.83 m (6.0 ft) in diameter and has an auxiliary rotor which is capable of rolling the flow to simulate a rolling aircraft. The former test section was used for all the tests conducted for this effort.

The tunnel is powered by a 600 HP electric motor which drives an 8 bladed 4.27 m (14.0 ft) diameter propeller. Dynamic pressures in excess of 1900 N/m^2 (39.7 lb/ft^2) can be obtained in the test section with no blockage.

Several balance systems are available for aircraft model testing. A strut supported mechanical balance was originally designed for the tunnel; it is still in use. A strut supported strain gage system is also available. A sting supported strain gage system can be used, but with

a large vertical pylon to support the unit. This mechanism creates enough tunnel blockage to reduce the maximum test section dynamic pressure to 1650 N/m^2 (34.5 lb/ft^2). All force and moment data were recorded with this balance.

APPENDIX B

ERROR ANALYSIS

All errors were estimated using accuracy data obtained from information supplied by the manufacturers of the various equipment used. Errors were computed for a representative set of test data; these were:

angle of attack	4.00	deg		±0.208%
dynamic pressure	300	N/m^2	(6.27 lb/ft^2)	±1.67%
wing area	0.113	m^2	(1.22 ft^2)	±0.00052%
wing span	1.20	m	(3.94 ft)	±0.097%
wing chord	0.0943	m	(0.309 ft)	±0.539%
Axial Force	1.60	N	(0.36 lb)	±5.63
Side Force	0.32	N	(0.072 lb)	±28.1%
Normal Force	12.0	N	(2.70 lb)	±0.75%
Rolling Moment	-0.400	Nm	(0.295 lb-ft)	±6.88%
Pitching Moment	0.700	Nm	(0.516 lb-ft)	±3.93%
Yawing Moment	0.100	Nm	(0.074 lb-ft)	±27.5%
Strain	300	μcm/cm		±0.67%

Force and moment accuracy estimates include balance, recording, and reading errors.

The Square Root of the Sum of the Squares Method was used to compute the errors in the lift, pitching, and rolling moment coefficients around the standard test condition. This method computes the error in some function F(x) by:

$$\Delta F = \left[\left(\frac{\partial F}{\partial x_1} \Delta x_1 \right)^2 + \left(\frac{\partial F}{\partial X_2} \Delta x_2 \right)^2 + \ldots \right]^{1/2}$$

The coefficients were computed from the standard equations:

$$C_m = \frac{m}{qSc}$$

$$C_\ell = \frac{\ell}{qSb}$$

$$C_L = C_X \sin\alpha - C_Z \cos\alpha$$

where

$$C_X = \frac{X}{qS}$$

$$C_Z = \frac{Z}{qS}$$

The resulting errors were:

C_m	±4.26%
C_ℓ	±7.00%
C_L	±1.83%

The lift coefficient error is dominated by the normal force because of the small angle of attack; the error in this force is caused by several inaccuracies, the largest being the dynamic pressure reading (±1.67%). Fabrication and balance inaccuracies make up the remainder of the error. The rolling and pitching moment coefficients have larger errors due to the greater apparent inaccuracy of

the balance and the additional linear dimension used. The balance inaccuracy is somewhat artificial since it is based on the standard set of conditions where the moments are small compared to the normal force. This situation, however, is representative of the actual test conditions.

The balance error also includes another inaccuracy based on the data reduction method used. A straight-line least squares curve fit was used for the influence coefficient matrix. The calibration data, however, was slightly non-linear. In reality the curve fitting error could be reduced (or eliminated) by the use of a better curve fit. For convenience the linear fit was used; the error resulting from its use represents about half of the stated balance inaccuracy.

APPENDIX C

NUMERICAL DATA

The following tables include the results from the experimental data obtained from the various tests. The data is presented in its reduced form. All corrections that were made are included in the results.

TABLE C1
AERODYNAMIC DATA

AERODYNAMIC DATA FOR OBLIQUE WINGS

TEST	Q(N/M2)	CLIFT	CM	CL
WING 1		SWEEP= 0.DEG	ALPHA=4.DEG	
1	249.	3.549E-01	6.228E-02	-8.124E-05
2	274.	3.561E-01	6.295E-02	-8.008E-05
3	299.	3.771E-01	7.728E-03	9.077E-04
4	224.	4.083E-01	6.151E-02	-9.466E-05
5	199.	3.674E-01	5.190E-02	-8.568E-05
WING 5		SWEEP=30.DEG	ALPHA=4.DEG	
6	249.	5.447E-01	1.511E-01	-3.110E-02
7	199.	3.069E-01	7.287E-02	-7.516E-03
8	224.	3.853E-01	1.031E-01	-1.941E-02
9	174.	3.139E-01	6.199E-02	9.465E-04
10	149.	2.830E-01	3.672E-02	7.476E-03
WING 8		SWEEP=60.DEG	ALPHA=4.DEG	
11	249.	9.417E-02	-2.245E-01	9.505E-03
12	274.	1.189E-01	-1.978E-01	8.633E-03
13	299.	1.208E-01	-1.698E-01	7.913E-03
14	324.	1.284E-01	-1.465E-01	7.114E-03
15	349.	1.230E-01	-1.141E-01	5.074E-03
WING 11		SWEEP=60.DEG	ALPHA=4.DEG	
16	249.	2.591E-01	2.772E-01	-7.210E-03
17	274.	2.433E-01	3.885E-01	-1.089E-02
18	299.	2.945E-01	6.176E-01	-1.814E-02
19	324.	3.779E-01	8.550E-01	-2.666E-02
20	224.	1.887E-01	1.463E-01	-4.016E-03
WING 11		SWEEP=45.DEG	ALPHA=4.DEG	
21	249.	4.662E-01	5.745E-01	-2.989E-02
22	274.	4.886E-01	7.415E-01	-3.781E-02
23	299.	5.044E-01	8.897E-01	-4.579E-02
24	224.	4.172E-01	4.042E-01	-1.837E-02
25	199.	3.933E-01	2.423E-01	-9.327E-03
WING 11		SWEEP=30.DEG	ALPHA=4.DEG	
26	249.	3.457E-01	3.216E-01	-3.224E-02
27	274.	5.153E-01	3.616E-01	-3.954E-02
28	299.	5.309E-01	3.811E-01	-4.380E-02
29	224.	4.397E-01	2.695E-01	-2.552E-02
30	199.	4.425E-01	-2.419E-01	-1.344E-03

AERODYNAMIC DATA FOR OBLIQUE WINGS

TEST	Q(N/M2)	CLIFT	CM	CL
WING 11		SWEEP=15.DEG	ALPHA=4.DEG	
31	249.	3.965E-01	1.037E-01	-1.915E-02
32	274.	4.246E-01	1.139E-01	-2.392E-02
33	299.	4.398E-01	1.052E-01	-2.789E-02
34	324.	4.708E-01	1.042E-01	-3.053E-02
35	224.	4.069E-01	6.087E-02	-1.730E-02
WING 11		SWEEP= 0.DEG	ALPHA=4.DEG	
36	249.	3.663E-01	9.293E-02	1.166E-03
37	274.	3.753E-01	9.681E-02	1.320E-03
38	299.	3.787E-01	1.181E-01	1.501E-03
39	324.	3.853E-01	1.153E-01	1.744E-03
40	349.	3.928E-01	1.321E-01	1.952E-03
WING 14		SWEEP= 0.DEG	ALPHA=4.DEG	
41	373.	2.713E-01	7.188E-02	1.521E-03
42	498.	3.016E-01	1.229E-01	1.955E-03
43	622.	3.225E-01	1.581E-01	2.501E-03
44	747.	3.355E-01	1.813E-01	2.735E-03
45	797.	3.421E-01	1.912E-01	2.903E-03
WING 14		SWEEP=15.DEG	ALPHA=4.DEG	
46	249.	2.483E-01	6.903E-02	-5.972E-05
47	373.	2.740E-01	8.577E-02	-3.550E-03
48	498.	2.994E-01	1.066E-01	-7.423E-03
49	622.	3.316E-01	1.338E-01	-1.246E-02
50	747.	3.653E-01	1.495E-01	-1.866E-02
WING 14		SWEEP=30.DEG	ALPHA=4.DEG	
51	249.	2.534E-01	1.019E-01	-1.012E-03
52	373.	3.008E-01	1.379E-01	-4.579E-03
53	498.	3.408E-01	1.652E-01	-1.473E-02
54	622.	3.967E-01	1.902E-01	-2.629E-02
55	672.	4.189E-01	2.011E-01	-3.163E-02
WING 14		SWEEP=45.DEG	ALPHA=4.DEG	
56	249.	1.899E-01	7.000E-02	4.349E-04
57	373.	2.122E-01	9.961E-02	-3.541E-03
58	423.	2.297E-01	1.194E-01	-5.937E-03
59	498.	2.615E-01	1.470E-01	-1.042E-02
60	573.	2.994E-01	1.811E-01	-1.612E-02

AERODYNAMIC DATA FOR OBLIQUE WINGS

TEST	Q(N/M2)	CLIFT	CM	CL
WING 14	SWEEP=60.DEG	ALPHA=4.DEG		
61	249.	1.260E-01	3.881E-02	4.465E-04
62	373.	1.346E-01	6.758E-02	-8.256E-04
63	498.	1.872E-01	9.991E-02	-3.021E-03
64	573.	1.713E-01	1.306E-01	-3.353E-03
65	622.	1.818E-01	1.499E-01	-5.758E-03
WING 17	SWEEP=60.DEG	ALPHA=4.DEG		
66	249.	1.094E-01	2.893E-02	6.892E-04
67	373.	1.173E-01	1.223E-01	-1.138E-03
68	498.	1.265E-01	1.032E-01	-3.124E-03
69	622.	1.513E-01	3.445E-01	-6.607E-03
70	672.	1.775E-01	4.557E-01	-9.742E-03
WING 17	SWEEP=45.DEG	ALPHA=4.DEG		
71	249.	1.952E-01	7.122E-02	1.144E-03
72	373.	2.081E-01	1.862E-01	-4.019E-03
73	498.	2.479E-01	3.376E-01	-1.197E-02
74	622.	3.633E-01	6.835E-01	-3.305E-02
75	647.	3.816E-01	7.643E-01	-3.719E-02
WING 17	SWEEP=30.DEG	ALPHA=4.DEG		
76	249.	3.131E-01	1.606E-01	8.776E-04
77	373.	2.875E-01	2.213E-01	-7.532E-03
78	498.	3.487E-01	3.333E-01	-2.176E-02
79	622.	4.145E-01	4.351E-01	-3.764E-02
80	672.	4.270E-01	4.608E-01	-4.235E-02
WING 17	SWEEP=15.DEG	ALPHA=4.DEG		
81	249.	3.429E-01	1.774E-01	-1.275E-03
82	373.	3.382E-01	1.724E-01	-6.594E-03
83	498.	3.499E-01	1.707E-01	-1.259E-02
84	622.	3.773E-01	1.713E-01	-1.991E-02
85	672.	3.838E-01	1.702E-01	-2.197E-02
WING 17	SWEEP= 0.DEG	ALPHA=4.DEG		
86	249.	3.783E-01	1.519E-01	3.718E-03
87	373.	3.929E-01	1.627E-01	5.933E-03
88	498.	4.012E-01	1.767E-01	7.993E-03
89	622.	4.178E-01	1.929E-01	8.939E-03
90	747.	4.151E-01	9.581E-01	8.356E-03

AERODYNAMIC DATA FOR OBLIQUE WINGS

TEST	Q(N/M2)	CLIFT	CM	CL
WING 2		SWEEP= 0.DEG	ALPHA=4.DEG	
91	199.	3.573E-01	2.199E-01	2.009E-03
92	224.	3.530E-01	2.267E-01	2.043E-03
93	249.	3.617E-01	2.325E-01	2.306E-03
94	274.	3.665E-01	2.416E-01	3.170E-03
95	299.	3.684E-01	5.955E-02	3.494E-03
WING 3		SWEEP= 0.DEG	ALPHA=4.DEG	
96	199.	3.168E-01	1.980E-01	1.630E-02
97	224.	3.300E-01	2.153E-01	1.712E-02
98	249.	3.404E-01	2.227E-01	1.802E-02
99	274.	3.405E-01	2.304E-01	1.709E-02
100	299.	3.493E-01	2.381E-01	1.820E-02
WING 4		SWEEP= 0.DEG	ALPHA=4.DEG	
101	199.	3.717E-01	2.676E-01	2.849E-02
102	224.	3.486E-01	2.777E-01	2.824E-02
103	249.	3.570E-01	2.871E-01	2.874E-02
104	274.	3.639E-01	2.948E-01	2.915E-02
105	299.	3.451E-01	2.922E-01	2.830E-02
WING 6		SWEEP=30.DEG	ALPHA=4.DEG	
106	149.	1.917E-01	5.271E-02	1.424E-02
107	174.	1.991E-01	7.847E-02	1.323E-02
108	199.	1.872E-01	1.027E-01	8.898E-03
109	224.	2.522E-01	1.249E-01	3.125E-03
110	249.	3.082E-01	1.633E-01	-7.211E-03
WING 7		SWEEP=30.DEG	ALPHA=4.DEG	
111	149.	1.944E-01	9.534E-02	3.370E-02
112	174.	1.903E-01	1.074E-01	3.195E-02
113	199.	1.782E-01	1.027E-01	3.033E-02
114	224.	1.826E-01	1.085E-01	2.802E-02
115	249.	1.811E-01	1.176E-01	2.664E-02
WING 9		SWEEP=60.DEG	ALPHA=4.DEG	
116	249.	9.503E-02	-2.837E-03	9.751E-03
117	274.	9.734E-02	7.622E-03	9.295E-03
118	299.	9.926E-02	1.631E-02	8.917E-03
119	324.	1.011E-01	1.776E-02	8.228E-03
120	349.	1.025E-01	2.388E-02	7.638E-03

AERODYNAMIC DATA FOR OBLIQUE WINGS

TEST	Q(N/M2)	CLIFT	CM	CL
WING 10	SWEEP=60.DEG		ALPHA=4.DEG	
121	249.	9.266E-02	2.338E-04	9.515E-03
122	274.	9.528E-02	1.002E-02	8.864E-03
123	299.	9.331E-02	1.566E-02	8.521E-03
124	324.	8.786E-02	1.777E-02	8.232E-03
125	349.	8.850E-02	2.174E-02	7.812E-03
WING 12	SWEEP= 0.DEG		ALPHA=4.DEG	
126	249.	3.684E-01	1.252E-01	1.182E-02
127	274.	3.790E-01	1.295E-01	1.247E-02
128	299.	3.901E-01	1.259E-01	1.221E-02
129	324.	3.992E-01	1.295E-01	1.273E-02
130	349.	4.020E-01	1.264E-01	1.249E-02
WING 12	SWEEP=15.DEG		ALPHA=4.DEG	
131	224.	3.515E-01	7.723E-02	-4.054E-03
132	249.	3.662E-01	7.772E-02	-6.757E-03
133	274.	3.832E-01	7.105E-02	-1.114E-02
134	299.	4.057E-01	7.772E-02	-1.598E-02
135	324.	4.307E-01	6.277E-02	-2.117E-02
WING 12	SWEEP=30.DEG		ALPHA=4.DEG	
136	199.	3.657E-01	1.073E-01	-7.534E-03
137	224.	4.125E-01	1.342E-01	-1.916E-02
138	249.	4.420E-01	1.493E-01	-2.631E-02
139	274.	4.629E-01	5.479E-01	-3.428E-02
140	299.	5.319E-01	8.456E-01	-4.233E-02
WING 12	SWEEP=45.DEG		ALPHA=4.DEG	
141	199.	2.684E-01	1.068E-01	-7.808E-03
142	224.	3.032E-01	1.577E-01	-1.463E-02
143	249.	3.742E-01	2.446E-01	-2.701E-02
144	274.	4.164E-01	3.403E-01	-3.735E-02
145	299.	4.493E-01	4.122E-01	-4.557E-02
WING 12	SWEEP=60.DEG		ALPHA=4.DEG	
146	224.	1.742E-01	9.160E-02	-2.424E-03
147	249.	1.917E-01	1.329E-01	-4.809E-03
148	274.	2.197E-01	1.836E-01	-7.848E-03
149	299.	2.621E-01	2.694E-01	-1.336E-02
150	324.	3.257E-01	3.877E-01	-2.207E-02

AERODYNAMIC DATA FOR OBLIQUE WINGS

TEST	Q(N/M2)	CLIFT	CM	CL
WING 13	SWEEP= 0.DEG	ALPHA=4.DEG		
151	249.	3.330E-01	2.313E-01	3.041E-02
152	274.	3.353E-01	2.499E-01	3.045E-02
153	299.	3.452E-01	2.673E-01	3.148E-02
154	324.	3.461E-01	2.703E-01	3.180E-02
155	349.	3.505E-01	2.803E-01	3.207E-02
WING 13	SWEEP=15.DEG	ALPHA=4.DEG		
156	224.	2.435E-01	9.735E-02	1.582E-02
157	249.	2.610E-01	1.010E-01	1.375E-02
158	274.	2.689E-01	1.133E-01	1.076E-02
159	299.	2.839E-01	1.267E-01	7.873E-03
160	324.	3.007E-01	1.349E-01	8.962E-03
WING 13	SWEEP=30.DEG	ALPHA=4.DEG		
161	199.	2.824E-01	1.372E-01	8.868E-03
162	224.	2.923E-01	1.459E-01	6.285E-03
163	249.	3.135E-01	1.633E-01	4.043E-04
164	274.	3.472E-01	1.810E-01	-7.659E-03
165	299.	3.991E-01	2.209E-01	-2.113E-02
WING 13	SWEEP=45.DEG	ALPHA=4.DEG		
166	199.	1.878E-01	6.312E-02	6.208E-03
167	224.	2.028E-01	8.395E-02	3.923E-03
168	249.	2.252E-01	1.071E-01	-5.240E-05
169	274.	2.871E-01	1.664E-01	-8.729E-03
170	299.	3.626E-01	2.466E-01	-2.272E-02
WING 13	SWEEP=60.DEG	ALPHA=4.DEG		
171	224.	1.488E-01	6.141E-02	2.083E-03
172	249.	1.461E-01	5.524E-02	1.871E-03
173	274.	1.556E-01	9.377E-02	-2.531E-04
174	299.	1.677E-01	1.169E-01	-2.224E-03
175	324.	1.931E-01	1.500E-01	-5.178E-03
WING 15	SWEEP= 0.DEG	ALPHA=4.DEG		
176	373.	3.361E-01	8.231E-02	-2.372E-02
177	498.	3.616E-01	8.141E-02	-2.188E-02
178	622.	3.797E-01	8.172E-02	-2.286E-02
179	747.	3.892E-01	1.104E-01	-2.304E-02
180	797.	3.946E-01	1.201E-01	-2.317E-02

AERODYNAMIC DATA FOR OBLIQUE WINGS

TEST	Q(N/M2)	CLIFT	CM	CL
WING 15	SWEEP=15.DEG		ALPHA=4.DEG	
181	249.	3.418E-01	1.351E-02	-1.938E-02
182	373.	3.463E-01	1.336E-02	-1.692E-02
183	498.	3.555E-01	2.257E-02	-1.439E-02
184	622.	3.653E-01	3.557E-02	-1.095E-02
185	747.	3.724E-01	5.193E-02	-6.999E-03
WING 15	SWEEP=30.DEG		ALPHA=4.DEG	
186	249.	2.654E-01	-5.785E-02	-1.674E-02
187	373.	2.868E-01	-3.280E-02	-1.309E-02
188	498.	2.871E-01	-6.490E-03	-9.360E-03
189	622.	3.029E-01	3.484E-02	-3.695E-03
190	672.	3.232E-01	6.134E-02	-7.859E-04
WING 15	SWEEP=45.DEG		ALPHA=4.DEG	
191	249.	2.359E-01	-9.017E-02	-1.173E-02
192	373.	2.375E-01	-6.327E-02	-9.585E-03
193	423.	2.398E-01	-5.176E-02	-8.464E-03
194	498.	2.444E-01	-1.573E-02	-7.803E-03
195	573.	2.512E-01	1.139E-03	-4.418E-03
WING 15	SWEEP=60.DEG		ALPHA=4.DEG	
196	249.	1.014E-01	-8.633E-02	-5.741E-03
197	373.	1.135E-01	-6.647E-02	-4.950E-03
198	498.	1.205E-01	-3.973E-02	-3.840E-03
199	573.	1.239E-01	-2.047E-02	-3.033E-03
200	622.	2.259E-01	-1.003E-02	-2.532E-03
WING 16	SWEEP= 0.DEG		ALPHA=4.DEG	
201	373.	4.062E-01	5.887E-02	-2.869E-02
202	498.	4.110E-01	7.650E-02	-2.940E-02
203	622.	4.177E-01	8.004E-02	-2.992E-02
204	747.	4.263E-01	8.125E-02	-3.027E-02
205	797.	4.293E-01	8.212E-02	-3.047E-02
WING 16	SWEEP=15.DEG		ALPHA=4.DEG	
206	249.	2.739E-01	8.200E-02	2.614E-02
207	373.	3.115E-01	7.972E-02	2.359E-02
208	498.	3.372E-01	7.844E-02	2.028E-02
209	622.	3.235E-01	7.823E-02	1.640E-02
210	747.	3.648E-01	7.685E-02	1.182E-02

AERODYNAMIC DATA FOR OBLIQUE WINGS

TEST	Q(N/M2)	CLIFT	CM	CL
WING 16	SWEEP=30.DEG	ALPHA=4.DEG		
211	249.	2.333E-01	-1.082E-02	2.257E-02
212	373.	2.603E-01	-2.819E-02	2.160E-03
213	498.	2.735E-01	-5.607E-03	1.601E-03
214	622.	2.994E-01	3.884E-02	7.644E-03
215	672.	3.069E-01	5.067E-02	4.601E-03
WING 16	SWEEP=45.DEG	ALPHA=4.DEG		
216	249.	2.160E-01	-7.771E-02	1.424E-02
217	373.	2.249E-01	-5.236E-02	1.170E-02
218	423.	2.273E-01	-3.782E-02	1.045E-02
219	498.	2.300E-01	-2.049E-02	8.639E-03
220	573.	2.376E-01	3.755E-03	6.157E-03
WING 16	SWEEP=60.DEG	ALPHA=4.DEG		
221	249.	1.986E-01	-8.460E-02	6.622E-03
222	373.	1.776E-01	-5.641E-02	5.674E-03
223	498.	1.637E-01	-3.519E-02	4.367E-03
224	573.	1.668E-01	-1.465E-02	3.481E-03
225	622.	1.604E-01	-1.736E-03	2.820E-03
WING 18	SWEEP= 0.DEG	ALPHA=4.DEG		
226	249.	4.117E-01	1.451E-01	1.705E-02
227	373.	4.110E-01	1.505E-01	1.943E-02
228	498.	4.229E-01	1.593E-01	2.109E-02
229	622.	3.882E-01	3.433E-01	2.195E-02
230	672.	3.731E-01	5.251E-01	2.810E-02
WING 18	SWEEP=15.DEG	ALPHA=4.DEG		
231	249.	3.099E-01	7.938E-02	1.136E-02
232	373.	3.244E-01	7.997E-02	5.953E-03
233	498.	3.449E-01	7.856E-02	3.968E-04
234	622.	3.421E-01	7.700E-02	-5.611E-03
235	672.	3.602E-01	7.976E-02	-8.294E-03
WING 18	SWEEP=30.DEG	ALPHA=4.DEG		
236	249.	2.420E-01	3.799E-02	9.469E-03
237	373.	2.304E-01	5.613E-02	4.231E-03
238	498.	2.573E-01	8.179E-02	-1.612E-03
239	622.	2.918E-01	1.112E-01	-1.112E-02
240	672.	3.103E-01	1.405E-01	-1.576E-03

AERODYNAMIC DATA FOR OBLIQUE WINGS

TEST	Q(N/M2)	CLIFT	CM	CL
WING 18	SWEEP=45.DEG	ALPHA=4.DEG		
241	249.	1.935E-01	-7.334E-03	7.337E-03
242	373.	1.829E-01	3.106E-02	4.401E-03
243	498.	1.830E-01	6.064E-02	1.027E-03
244	622.	1.934E-01	9.582E-02	-2.811E-03
245	672.	2.004E-01	1.122E-01	-4.460E-03
WING 18	SWEEP=60.DEG	ALPHA=4.DEG		
246	249.	1.297E-01	-4.317E-02	4.735E-03
247	373.	1.128E-01	-1.699E-02	3.308E-03
248	498.	1.090E-01	1.121E-02	2.356E-03
249	622.	1.068E-01	1.760E-02	1.308E-03
250	672.	1.090E-01	4.123E-02	8.561E-04
WING 19	SWEEP= 0.DEG	ALPHA=4.DEG		
251	249.	4.064E-01	1.537E-01	1.800E-02
252	373.	4.086E-01	1.643E-01	2.197E-02
253	498.	4.131E-01	1.649E-01	2.229E-02
254	622.	3.940E-01	4.445E-01	2.275E-02
255	672.	3.812E-01	5.886E-01	2.283E-02
WING 19	SWEEP=15.DEG	ALPHA=4.DEG		
256	249.	3.372E-01	8.557E-02	1.087E-02
257	373.	3.329E-01	8.028E-02	6.111E-03
258	498.	3.374E-01	7.981E-02	1.106E-03
259	622.	3.436E-01	7.766E-02	-3.707E-03
260	672.	3.478E-01	7.687E-02	-5.645E-03
WING 19	SWEEP=30.DEG	ALPHA=4.DEG		
261	249.	2.799E-01	3.537E-02	4.219E-03
262	373.	2.790E-01	6.358E-02	-5.449E-04
263	498.	2.855E-01	8.868E-02	-6.383E-03
264	622.	3.050E-01	1.151E-01	-1.351E-02
265	672.	3.209E-01	1.294E-01	-1.755E-02
WING 19	SWEEP=45.DEG	ALPHA=4.DEG		
266	249.	2.089E-01	9.497E-03	5.190E-03
267	373.	2.100E-01	5.295E-02	1.220E-03
268	498.	2.212E-01	9.862E-02	-3.746E-03
269	622.	2.576E-01	1.656E-01	-1.159E-02
270	672.	2.795E-01	2.020E-01	-1.489E-02

AERODYNAMIC DATA FOR OBLIQUE WINGS

TEST	Q(N/M2)	CLIFT	CM	CL
WING 19	SWEEP=60.DEG		ALPHA=0.DEG	
271	249.	1.398E-01	4.744E-03	2.587E-03
272	373.	1.163E-01	3.912E-02	1.243E-03
273	498.	1.357E-01	7.336E-02	-5.088E-04
274	622.	1.436E-01	1.103E-01	-2.416E-03
275	672.	1.507E-01	1.292E-01	-3.565E-03
WING 20	SWEEP= 0.DEG		ALPHA=4.DEG	
276	199.	3.176E-01	2.717E-01	2.022E-03
277	249.	3.251E-01	2.909E-01	2.081E-03
278	299.	3.321E-01	3.040E-01	2.318E-03
279	373.	3.440E-01	3.040E-01	2.316E-03
280	423.	3.540E-01	3.094E-01	2.314E-03
WING 20	SWEEP=15.DEG		ALPHA=4.DEG	
281	199.	3.177E-01	2.107E-01	1.719E-03
282	249.	3.309E-01	2.126E-01	-1.023E-03
283	299.	3.462E-01	2.172E-01	-4.242E-03
284	373.	3.684E-01	2.132E-01	-9.666E-03
285	423.	3.913E-01	2.153E-01	-1.367E-02
WING 20	SWEEP=30.DEG		ALPHA=4.DEG	
286	199.	2.852E-01	1.901E-01	-2.443E-03
287	249.	2.959E-01	2.406E-01	1.127E-03
288	299.	3.227E-01	2.304E-01	6.292E-03
289	373.	3.705E-01	2.824E-01	1.723E-02
290	423.	4.027E-01	3.146E-01	2.555E-02
WING 20	SWEEP=45.DEG		ALPHA=4.DEG	
291	199.	2.086E-01	1.329E-01	-3.021E-03
292	249.	2.180E-01	1.504E-01	-9.987E-04
293	299.	2.339E-01	1.764E-01	1.933E-03
294	349.	2.535E-01	2.251E-01	5.727E-03
295	398.	2.917E-01	2.460E-01	1.184E-02
WING 20	SWEEP=60.DEG		ALPHA=4.DEG	
296	199.	1.318E-01	8.587E-02	-2.707E-03
297	249.	1.347E-01	9.721E-02	-1.696E-03
298	373.	1.480E-01	1.183E-01	4.431E-04
299	423.	1.575E-01	1.353E-01	1.785E-03
300	498.	1.854E-01	1.802E-01	5.078E-03

AERODYNAMIC DATA FOR OBLIQUE WINGS

TEST	Q(N/M2)	CLIFT	CM	CL
WING 23	SWEEP= 0.DEG	ALPHA=4.DEG		
301	199.	3.665E-01	2.609E-01	3.199E-03
302	249.	3.738E-01	2.809E-01	3.733E-03
303	299.	3.788E-01	2.838E-01	3.893E-03
304	373.	3.942E-01	3.034E-01	4.524E-03
305	398.	3.969E-01	3.063E-01	4.384E-03
WING 23	SWEEP=15.DEG	ALPHA=4.DEG		
306	199.	5.426E-01	2.291E-01	-1.215E-04
307	249.	3.764E-01	2.277E-01	-6.036E-03
308	299.	4.056E-01	2.157E-01	-1.299E-02
309	349.	4.415E-01	2.074E-01	-2.187E-02
310	373.	4.558E-01	1.997E-01	-2.598E-02
WING 23	SWEEP=30.DEG	ALPHA=4.DEG		
311	174.	2.927E-01	2.069E-01	5.345E-03
312	224.	3.247E-01	2.066E-01	-2.714E-03
313	249.	3.449E-01	2.142E-01	-7.457E-03
314	299.	4.141E-01	2.206E-01	-2.292E-02
315	324.	4.333E-01	2.525E-01	-2.941E-02
WING 23	SWEEP=45.DEG	ALPHA=4.DEG		
316	149.	2.180E-01	1.181E-01	7.894E-03
317	199.	2.313E-01	1.340E-01	4.715E-03
318	249.	2.523E-01	1.516E-01	-2.934E-04
319	299.	3.086E-01	1.893E-01	-9.996E-03
320	349.	4.038E-01	2.801E-01	-2.919E-02
WING 23	SWEEP=60.DEG	ALPHA=4.DEG		
321	199.	1.302E-01	6.695E-02	3.544E-03
322	249.	1.336E-01	7.387E-02	2.591E-03
323	299.	1.420E-01	8.925E-02	1.557E-03
324	349.	1.572E-01	1.073E-01	-7.163E-04
325	398.	1.983E-01	1.567E-01	-5.258E-03
WING 26	SWEEP= 0.DEG	ALPHA=4.DEG		
326	199.	3.854E-01	2.241E-01	1.998E-03
327	249.	3.791E-01	2.428E-01	2.298E-03
328	299.	3.852E-01	2.524E-01	2.496E-03
329	373.	4.061E-01	2.630E-01	2.610E-03
330	423.	3.957E-01	2.715E-01	2.717E-03

AERODYNAMIC DATA FOR OBLIQUE WINGS

TEST	Q(N/M2)	CLIFT	CM	CL
WING 26	SWEEP=15.DEG		ALPHA=4.DEG	
331	199.	3.640E-01	2.133E-01	9.108E-04
332	249.	3.679E-01	2.104E-01	-2.227E-03
330	299.	3.812E-01	2.171E-01	-5.842E-03
334	349.	4.155E-01	2.172E-01	-9.622E-03
335	398.	4.156E-01	2.163E-01	-1.424E-02
WING 26	SWEEP=30.DEG		ALPHA=4.DEG	
336	199.	3.144E-01	1.392E-01	2.962E-03
337	249.	3.604E-01	1.658E-01	-1.992E-03
338	299.	3.677E-01	1.878E-01	-9.217E-03
339	349.	4.162E-01	2.134E-01	-1.983E-02
340	373.	4.392E-01	2.263E-01	-2.519E-02
WING 26	SWEEP=45.DEG		ALPHA=4.DEG	
341	199.	2.097E-01	9.717E-02	3.525E-03
342	249.	2.440E-01	1.170E-01	1.612E-03
343	299.	2.635E-01	1.519E-01	-2.045E-03
344	349.	3.027E-01	2.076E-01	-8.065E-03
345	398.	3.723E-01	2.940E-01	-2.018E-02
WING 26	SWEEP=60.DEG		ALPHA=4.DEG	
346	199.	1.484E-01	6.236E-02	3.241E-03
347	299.	1.519E-01	8.995E-02	1.959E-03
348	349.	1.567E-01	1.052E-01	8.163E-04
349	398.	1.665E-01	1.374E-01	-4.824E-04
350	473.	1.954E-01	2.053E-01	-4.179E-03

TABLE C2

STRAIN DATA

TEST	$q(N/m^2)$		$\varepsilon(\mu cm/cm)$
Wing 1	$\Lambda=0°$	$\alpha=4°$	
1	249		326
2	274		366
3	299		401
4	224		291
5	199		261
Wing 5	$\Lambda=30°$	$\alpha=4°$	
6	249		540
7	199		275
8	224		400
9	174		200
10	149		140
Wing 8	$\Lambda=60°$	$\alpha=4°$	
11	249		66
12	274		81
13	299		97
14	324		121
15	349		171
Wing 11	$\Lambda=60°$	$\alpha=4°$	
16	249		184
17	274		234
18	299		354
19	324		474
20	224		141
Wing 11	$\Lambda=45°$	$\alpha=4°$	
21	249		389
22	274		504
23	299		614
24	224		284
25	199		204
Wing 11	$\Lambda=30°$	$\alpha=4°$	
26	249		392
27	274		494
28	299		564
29	224		334
30	199		246

TABLE C2 - STRAIN DATA - continued

TEST	$q(N/m^2)$		$\varepsilon(\mu cm/cm)$
Wing 11	$\Lambda=15°$	$\alpha=4°$	
31	249		322
32	274		374
33	299		434
34	324		484
35	224		272
Wing	$\Lambda=0°$	$\alpha=4°$	
36	249		254
37	274		269
38	299		299
39	324		327
40	349		354
Wing 14	$\Lambda=0°$	$\alpha=4°$	
41	373		110
42	498		140
43	622		180
44	747		225
45	797		240
Wing 14	$\Lambda=15°$	$\alpha=4°$	
46	249		70
47	373		118
48	498		176
49	622		240
50	747		310
Wing 14	$\Lambda=30°$	$\alpha=4°$	
51	249		77
52	373		125
53	498		195
54	622		292
55	672		340
Wing 14	$\Lambda=45°$	$\alpha=4°$	
56	249		60
57	373		100
58	423		120
59	498		155
60	573		200

TABLE C2 - STRAIN DATA - continued

TEST	$q(N/m^2)$		$\varepsilon(\mu cm/cm)$
Wing 14	$\Lambda=60°$	$\alpha=40$	
61	249		40
62	373		60
63	498		97
64	573		119
65	622		140
Wing 17	$\Lambda=60°$	$\alpha=40$	
66	249		30
67	373		50
68	498		80
69	622		140
70	672		185
Wing 17	$\Lambda=45°$	$\alpha=4°$	
71	249		50
72	373		90
73	498		160
74	622		345
75	647		390
Wing 17	$\Lambda=30°$	$\alpha=4°$	
76	249		70
77	373		120
78	498		220
79	622		370
80	672		420
Wing 17	$\Lambda=15°$	$\alpha=4°$	
81	249		80
82	373		135
83	498		200
84	622		285
85	672		323
Wing 17	$\Lambda=0°$	$\alpha=4°$	
86	249		88
87	373		135
88	498		188
89	622		240
90	747		292

TABLE C2 - STRAIN DATA - continued

TEST	$q(N/m^2)$			$\varepsilon(\mu cm/cm)$
Wing 13	$\Lambda=45°$	$\alpha=4°$	(FREE TO ROLL)	
401	249			170
402	274			140
403	299			132
404	349			120
405	373			112
406	398			115
407	423			120
408	448			120
409	473			121
410	498			120
Wing 13	$\Lambda=45°$	$\alpha=4°$	(CLAMPED)	
411	249			180
472	274			290
413	299			435
414	324			590
415	349			705
416	373			850
417	398			970
418	423			1150
419	448			1290
Wing 13	$\Lambda=30°$	$\alpha=4°$	(FREE TO ROLL)	
420	249			177
421	274			171
422	299			162
423	324			156
424	349			162
425	373			152
426	398			162
427	423			162
428	448			156
429	473			156
430	498			157
431	548			156
432	598			160
433	648			153
434	697			154
435	747			150
436	797			145
437	822			146
438	847			142

AN EXPERIMENTAL INVESTIGATION OF OBLIQUE WING STATIC AEROELASTIC PHENOMENA

by

Basil S. Papadales, Jr.

(ABSTRACT)

A series of wind tunnel tests were conducted to determine the aerodynamic forces and moments produced by several clamped oblique wings. The wing sweep and aileron deflection angles were varied throughout a wide range of dynamic pressures. The wing structure was also stiffened. Strains were measured in the swept forward wing panels.

Results from these tests showed that increasing the wing structural stiffness or applying aileron deflection would increase the wing divergence speed. The divergence speed decreased as the sweep angle increased.

Further tests were conducted with the wing unconstrained in roll. Results showed that an oblique wing will attempt to unload its sweptforward panel by assuming a banked position. The wings were found to flutter before unclamped divergence occurred. Finally, it was found that the wing loading of an oblique wing can remain constant for a given aileron deflection throughout a wide range of velocities including velocities above the clamped divergence speed.